Available online at www.sciencedirect.com
SCIENCE DIRECT®
ELSEVIER
Palaeogeography, Palaeoclimatology, Palaeoecology 206 (2004) 217–238
PALAEO
www.elsevier.com/locate/palaeo

Paleobiology and skeletochronology of Jurassic dinosaurs: implications from the histology and oxygen isotope compositions of bones

T. Tütken[a,*], H.-U. Pfretzschner[b], T.W. Vennemann[a], G. Sun[c], Y.D. Wang[c]

[a] *Institut de Minéralogie et Géochemie, Université de Lausanne, BFSH 2, 1015 Lausanne, Switzerland*
[b] *Institut für Geowissenschaften, Arbeitsbereich Biogeologie und Angewandte Paläontologie, Sigwartstrasse 10, Universität Tübingen, 72076 Tübingen, Germany*
[c] *Nanjing Institute of Geology and Palaeontology, Academia Sinica, 210008 Nanjing, PR China*

Received 23 July 2003; accepted 8 September 2003

Abstract

Fossil biogenic phosphate of fast-growing primary bone tissue of dinosaurs can preserve a histologic and isotopic time-series of annual seasonality in temperature variations, similar to tooth enamel and other accretionary skeletal phases such as corals or wood. On two bone fragments from sympatric dinosaurs with different histologic patterns of bone growth, high-resolution oxygen isotope profiles were analyzed along the radial direction of bone growth. The investigated specimens are from the Jurassic Shishugou Formation in the Junggar Basin, NW China and have distinct patterns of compositional variation. A fibrolamellar dinosaur bone with multiple lines of arrested growth (LAGs) and periodic growth cycles of decreasing bone laminae thickness displays a cyclic intra-bone variation in $\delta^{18}O$ values of about 2‰ corresponding with the LAGs. These growth cycles in fast-growing fibrolamellar bone provide evidence for seasonal growth of dinosaurs in lower latitudes ($\sim 45°N$), possibly influenced by a monsoon-type paleoclimate. Seasonal changes in temperature and water supply are consistent with the oxygen isotope composition measured in dinosaur bone phosphate as well as with growth rings in contemporaneous fossil conifer wood from the same locality. In contrast, a plexiform sympatric sauropod bone displays continuous growth, free of LAGs and has a lower intra-bone variation of ≤ 0.8‰. Differences in bone histology are also reflected in the oxygen isotopic composition and its intra-bone variability, indicating different physiological responses to external climatic stress between sympatric dinosaur species. Seasonal intra-bone oxygen isotope variations combined with bone histology may thus yield new insights into species-specific response to climatic stress and its influence on dinosaur growth, formation of growth marks, growth rates, as well as dinosaur thermophysiology.

Keywords: Dinosaur bone; Oxygen isotopes; Histology; Climate; Growth; Diagenesis

1. Introduction

Knowledge of how dinosaurs grew (e.g., Reid, 1997a; Erickson et al., 2001; Padian et al., 2001) is fundamental to our understanding of their means of

* Corresponding author. Tel.: +41-21-692-44-48; fax: +41-21-692-43-05.
E-mail address: thomas.tutken@img.unil.ch (T. Tütken).

0031-0182/$ - see front matter © 2004 Elsevier B.V. All rights reserved.
doi:10.1016/j.palaeo.2004.01.005

reproductivity, thermophysiology, and their evolutionary success that made them the prevailing land vertebrates for most of the Mesozoic (e.g., Farlow and Brett-Surman, 1997; Sereno, 1999). Indirect evidence from trackways (Lockley, 1994) and nesting sites (Horner and Currie, 1994) and especially comparison of bones and bone histology from different ontogenetic growth stages have provided insights into dinosaur growth and growth rates (Varricchio, 1993; de Ricqlès et al., 1998; Erickson and Tumanova, 2000; Horner et al., 2000; Erickson et al., 2001; Padian et al., 2001). Bone tissue provides the only direct record of the ontogenetic growth of these extinct vertebrates and its microstructure can give clues to multiple aspects of dinosaur paleobiology including growth rates (de Ricqlès, 1980; Reid, 1997a; Varricchio, 1997; Erickson et al., 2001; Sander and Tückmantel, 2003), longevity (de Ricqlès, 1983; Chinsamy, 1990; Varricchio, 1993), age at maturity (Chinsamy, 1990; Varricchio, 1993; Sander, 1999), anatomical function (de Buffrénil et al., 1986) and metabolism (de Ricqlès, 1974, 1980; Reid, 1997a,b). Besides histologic information about growth, bone tissue is also an archive for the chemical and isotopic composition of dietary intake and drinking water (Longinelli, 1984; Luz et al., 1984; Luz and Kolodny, 1985; Koch et al., 1994; Koch, 1998; Hoogewerff et al., 2001; Kohn and Cerling, 2002). Thus primary bone tissue with little or no remodeling can potentially preserve a time-series of climatic and dietary information along its radial axis of growth similar to that of tooth enamel (Fricke and O'Neil, 1996; Sharp and Cerling, 1998; Wilkinson and Ivany, 2002).

In this paper, we present first results of a pilot study combining the analysis of bone histology and high-resolution oxygen isotope composition of Jurassic dinosaur bones from the Junggar Basin in northwest China as a possible test for the annual formation of histologic growth marks like LAGs which are applied to determine the growth rates of dinosaurs (Curry, 1999; Sander, 1999; Erickson and Tumanova, 2000; Horner et al., 2000; Erickson et al., 2001). The discovery of LAGs within the dinosaur bones has opened up the question on whether or not these could be related to an extreme annual seasonality such as the monsoon climate known to have existed in Central Asia during the Jurassic as reflected in fossil wood from contemporary deposits in the Junggar Basin and in the vicinity of the basin (Keller and Hendrix, 1997; Wang et al., 2000).

1.1. Bone histology — a mirror of the growth history

Primary bone tissue is formed by mineralization of cartilageous bone tissue with biogenic apatite forming primary bone tissues of different histology, e.g., fibrolamellar bone, plexiform bone, lamello-zonal bone (see Figs. 1 and 2, and Francillon-Vieillot et al., 1990; Reid, 1997a for details). Primary bone tissue thus is an archive of the animals growth history and its histology and growth marks allow for the reconstruction of growth rates of extant and extinct vertebrates (e.g., Castanet et al., 1993; Sander, 1999; Erickson et al., 2001). Throughout the ontogeny, bone tissue of vertebrates can be remodeled (Enlow, 1963; Hancox, 1972; Frost, 1980; Jee, 1988). During this remodeling and secondary tissue deposition the primary bone histology and growth cycles formed earlier can be lost. This in vivo remodeling process takes place by bone resorption through osteoclast cells and reprecipitation by osteoblast cells (Enlow, 1963; Jee, 1988). As a result of this remodeling process, secondary osteons form and they are delaminated from the surrounding bone tissue by a characteristic highly mineralized cement line of apatite (Fig. 2c). This distinguishes them from primary osteons that lack such a cement line (Fig. 2b). The degree of bone remodeling is a function of the species, metabolic rate, bone tissue type, ontogenetic age and mechanical strain (Enlow, 1963; Hancox, 1972; Frost, 1980; Jee, 1988).

The diaphyses of dinosaur long bones are dominantly made up of primary "laminar fibrolamellar bone" (de Ricqlès, 1974; Francillon-Vieillot et al., 1990), which is a type of highly vascularized bone tissue typical of fast-growing vertebrates (de Ricqlès et al., 1991). This indicates a rapid and continuous ontogenetic growth of juvenile dinosaurs with growth rates similar to those of birds and mammals (Reid, 1990; Varricchio, 1993, 1997; Curry, 1999; Horner et al., 1999, 2000; Erickson et al., 2001; Padian et al., 2001). Dinosaurs combined the fast continuous growth of large endotherms with the indefinite periodic growth of reptiles (de Ricqlès, 1980; Reid, 1997a,b). Fibrolamellar bone without significant in vivo remodeling (see Section 2.1 and Fig. 2 for explanation) records nearly the entire growth history

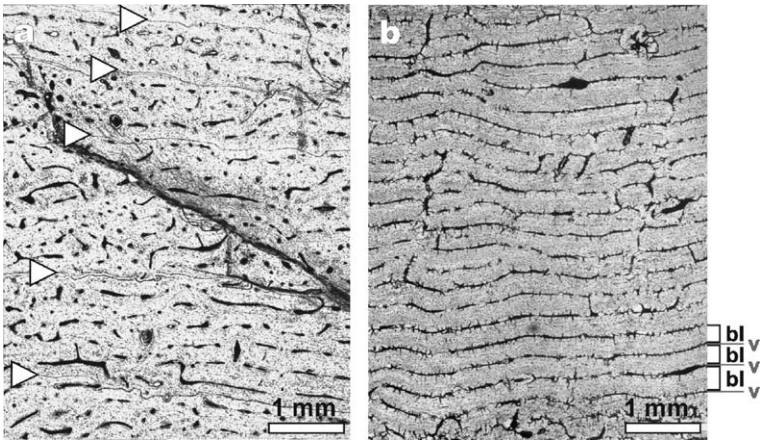

Fig. 1. (a) Photomicrograph of a sauropod bone showing multiple LAGs (white triangles) in a young adult fibrolamellar bone tissue indicating periodic stops of bone growth. The distance between LAGs decreases towards the cortex, probably reflecting decreasing growth rate. (b) Photomicrograph of a plexiform sauropod bone modified after Pfretzschner et al. (2001). The plexiform bone is made up of bone layers of similar thickness of around 250 μm (For illustration purposes three layers are marked with (bl) that are separated by small layers of high vascularized tissue (v). The bone histology without LAGs indicates continuous bone growth at a constant rate for this sauropod. In contrast to plexiform bones, layered bone structures are less well defined in fibrolamellar bones and were formed through alignment of primary osteons. The average distance between the central osteonal canals of two such subparallel "rows" of primary osteons are defined as a bone layer for the fibrolamellar bone. The bone layer thickness of both specimens was microscopically measured on thin sections and is given in Fig. 7.

of an individual dinosaur (Horner et al., 1999; Sander, 1999, 2000). Due to periodically slow growth rates or cessation of growth, some dinosaur bones show growth rings or growth lines (de Ricqlès, 1980, 1983; Reid, 1981, 1990; Chinsamy, 1990; Padian, 1997). Such growth lines are a common feature of many vertebrate bones, regardless of size or phylogenetic position (Castanet et al., 1993) and they also appear in teeth and bones of endothermic mammals (Klevezal and Kleinenberg, 1967; Buffrénil and Buffetaut, 1981; Buffrénil, 1982; Klevezal, 1996). Most frequently they are found in bones of ectothermic reptiles (Castanet and Smirina, 1990; Castanet et al., 1993) as result of the seasonal cyclicity of environmental conditions (e.g., cold–hot or dry–wet) (Peabody, 1961; Chinsamy et al., 1998; Horner et al., 1999). They are recorded in bone histology as bands of dense avascular tissue, so called annuli, or as lines of arrested growth (LAGs), representing finite time intervals where bone growth stopped temporarily and which mark the location of the surface during the growth pause. LAGs represent histological time markers of osteogenesis which may allow for the quantification of a time interval and the amount of bone growth within it. Given that the period of time between the LAG formation due to an endogenous or exogenous trigger mechanism can be estimated, bone and hence animal growth rates can be inferred (Castanet et al., 1993). This method of skeletochronology, which involves microscopic investigation of bone histology and cyclical growth marks, can also be applied to dinosaur bones allowing the quantification of growth rates and life histories of dinosaurs (Horner et al., 1997, 1999, 2000; Curry, 1999; Sander, 1999, 2000; Erickson et al., 2001; Padian et al., 2001; Sander and Tückmantel, 2003).

Dinosaur bones with multiple periodic LAGs potentially yield information on longevity and individual ages as well as growth rates and growth patterns (Horner et al., 1999; Sander and Tückmantel, 2003), if these are assumed to be of seasonal origin as commonly observed in living ectotherm vertebrates (Peabody, 1961; Hutton, 1986; Castanet and Smirina, 1990; Castanet et al., 1993). Thus the knowledge of the chronology of such growth marks is of crucial importance for skeletochronology and the assessment of accurate age estimates and growth rates for extinct

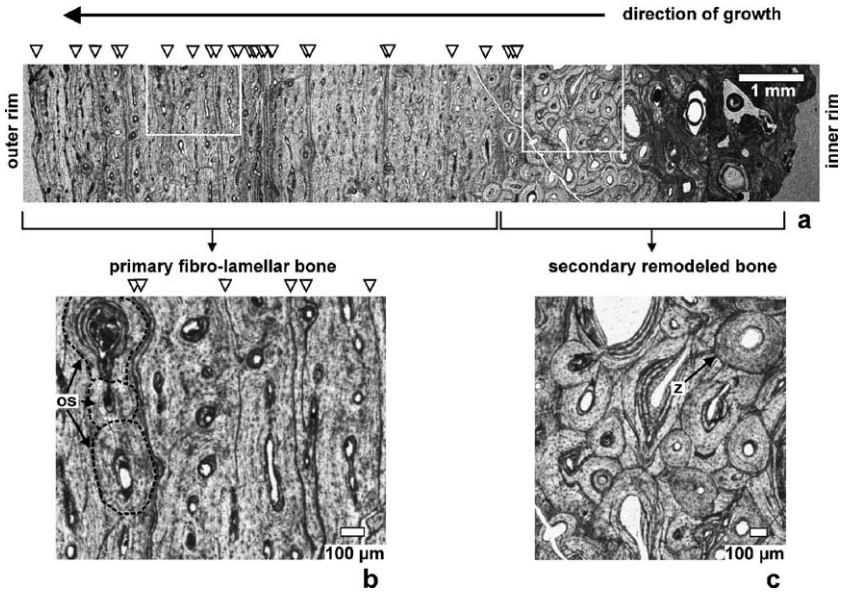

Fig. 2. (a) Photomicrograph of the cross section of the compacta of a fibrolamellar dinosaur bone from the same partial sauropod skeleton as the specimen in Fig. 1a. This specimen has at least 27 identifiable LAGs of irregular spacing (white triangles) situated in the tissue of the fibrolamellar bone. Fibrolamellar bone is formed by primary osteons (os) embedded in a matrix of woven bone. A primary osteon has a vascular canal in its center and is concentrically surrounded by osteonal bone laminae (b and Reid, 1997a). The white frames mark the two bone areas displayed in enlarged form in (b) and (c). The occurrence of remodeled Haversian bone (c) only at the inner rim indicates a sub-adult individual of Growth Stage A defined for the sauropod Apatosaurus according to Curry (1999). In contrast to a lack of LAGs in fibrolamellar bone of Growth Stage A (Curry, 1999), multiple LAGs indicating periodic interruptions in osteogenesis occur in the bone of this study. (b) The outer 2/3 of the bone cross section are made up of primary fibrolamellar bone without substantial bone remodeling that have preserved the histological growth structures such as primary osteons and LAGs. Three primary osteons are indicated by stippled black lines. LAGs circumvent these primary osteons as is typical for such primary growth marks in contrast to diagenetic cracks that tend to cut through histological structures. (c) The inner rim towards the marrow cavity has been intensively remodeled through the formation of secondary osteons, which are characterized by a sharp, higher mineralized cement line (z) of apatite surrounding each secondary osteon. Secondary osteons have destroyed the fibrolamellar bone tissue and its growth structures by cutting through the primary bone tissue and other secondary osteons, forming a so-called Haversian bone.

vertebrates. However, not all growth lines have the same structure and origin. The formation of LAGs may be caused by seasonal environmental effects like variations in temperature and humidity, or hormonal and physiological factors during the reproductive cycle, or hibernation as well as noncyclical events such as illness, starvation or singular extreme environmental factors like droughts (Peabody, 1958; Chinsamy, 1990; Castanet et al., 1993; Chinsamy et al., 1998; Reid, 1997a; Horner et al., 2000).

Multiple LAGs have frequently been observed in dinosaur bones of different genera (Reid, 1981, 1990; Chinsamy, 1990; Varricchio, 1993; Horner et al., 1999, 2000). Usually these LAGs are confined to the slow-growing external layer of poorly vascularized lamello-zonal bone which is formed after main ontogenetic growth when the animal has already approached maturity (Curry, 1999; Horner et al., 1999, 2000; Reid, 1990; Varricchio, 1993). An example of multiple annual LAGs in fibrolamellar dinosaur bone has been described from the Australian dinosaur *Timimus hermani* from polar paleolatitudes (Chinsamy, 1995; Chinsamy et al., 1998). As similar multiple LAGs in fibrolamellar bone are known from recent polar bears, Chinsamy et al. (1998) interpreted the LAGs in these dinosaurs from polar latitudes as annual growth cycles resulting from extreme climatic conditions during the polar winter. The formation of LAGs in other dinosaur species seems to be endogenously triggered as *Hypsilophodontides* from Cretaceous polar latitudes lack growth rings just like their counterparts from temperate lower latitudes, while in

contrast sympatric dinosaurs in both climate regimes have growth rings and LAGs (Chinsamy et al., 1998). Bone histology of sympatric dinosaur species indicates that they have reacted differently to climatic stress (Chinsamy et al., 1998). This may be due to different basal metabolic rates and thermophysiology making some species more susceptible to exogenous climatic influences on their metabolism and (bone) growth. Curry (1999) indicated that bones from *Apatosaurus* show growth cycles in the size of vascularization of primary compact bone, even in less seasonal climates. Environmental conditions such as temperature, precipitation and diet have an influence on growth rates and bone histology as observed in extant and fossil crocodiles (Buffrénil and Buffetaut, 1981; Hutton, 1986; Horner et al., 1999). Therefore, a climatic influence on the growth of dinosaurs seems likely and a seasonal or annual cyclicity may be recorded in bone histology.

1.2. Oxygen isotopes in bone phosphate — a proxy for seasonality of bone growth

The oxygen isotopic composition of skeletal apatite of extant and extinct terrestrial vertebrates is a proxy for continental paleoclimate (Longinelli, 1984, 1995; Koch, 1998; Kohn and Cerling, 2002). Seasonality in climate can also be recorded in the oxygen isotope composition of the phosphatic skeletal remains of vertebrates (Koch et al., 1989; Fricke and O'Neil, 1996; Fricke et al., 1998; Kohn et al., 1998; Sharp and Cerling, 1998; Barrick et al., 2001; Kohn and Cerling, 2002). High-resolution measurements of the oxygen isotope composition of phosphate ($\delta^{18}O_p$) from fast-growing primary bone tissue is therefore a promising tool to test the annual nature of histological growth marks like density of vascularization, annuli or LAGs. As body water is in oxygen isotope equilibrium with biogenic phosphate in animals (Pflug et al., 1979; Schoeller et al., 1986; Wong et al., 1988) the oxygen isotope composition of bone and teeth phosphate reflects that of the body fluid ($\delta^{18}O_{bw}$) and/or the (body) temperature during apatite formation (Longinelli and Nuti, 1973; Kolodny et al., 1983; Longinelli, 1984; Luz and Kolodny, 1989). Because of relatively constant body temperatures (± 2 °C) in homeotherms (Bligh and Johnson, 1973), $\delta^{18}O_p$ values are independent of ambient temperature, and H_2O-PO_4^{3-} fractionation (Longinelli and Nuti, 1973) in the animal during bone formation is constant. Hence, the oxygen isotope composition of bone and tooth phosphate from homeothermic mammals reflects $\delta^{18}O_{bw}$ values from which it has formed under equilibrium conditions (Kolodny et al., 1983; Longinelli, 1984). For large homeothermic animals, $\delta^{18}O_{bw}$ depends mainly on the $\delta^{18}O$ values of the meteoric water ingested during drinking and eating as well as their physiology and metabolic rate (Luz et al., 1984; Luz and Kolodny, 1985; Bryant and Froelich, 1995; Kohn, 1996). The $\delta^{18}O$ values of ingested meteoric water, in turn, are a function of mean annual air temperature and humidity, and hence of the prevailing climate (Dansgaard, 1964; Rozanski et al., 1993; Fricke and O'Neil, 1999). Thus $\delta^{18}O_p$ values of bones and teeth incorporated during biomineralization reflect seasonal variations of ambient temperature and fluid isotopic composition and can be used as a proxy for paleoclimate and drinking water consumption (Longinelli, 1984, 1995; Fricke and O'Neil, 1996; Fricke et al., 1998; Sharp and Cerling, 1998; Tütken et al., 2002; Wilkinson and Ivany, 2002). Biogenic phosphate in primary skeletal tissues without significant in vivo remodeling can preserve along their growth axis an isotopic time-series of annual climate seasonality (Fig. 3) and dietary intake (Fricke and O'Neil, 1996; Fricke et al., 1998; Koch, 1998; Kohn et al., 1998; Balasse et al., 1999, 2002; Passey and Cerling, 2002; Wilkinson and Ivany, 2002). If preserved in fossil bones, it can be used as a proxy for climate seasonality and as a time marker which allows for independent testing of the assumed annual nature of LAGs and other growth marks. This would improve the method of skeletochronology (Castanet et al., 1993) significantly and allow us to infer ontogenetic ages, the amount of annual bone apposition and thus dinosaur growth rates.

$\delta^{18}O_p$ values of bones may also provide information on the animal's metabolic rate (Bryant and Froelich, 1995; Kohn, 1996) and thermophysiology (Barrick and Showers, 1994; Barrick et al., 1996, 1997; Fricke and Rogers, 2000; Stoskopf et al., 2001; Showers et al., 2002). Low intra- and inter-bone variability (<1 ‰) in $\delta^{18}O_p$ values of dinosaur bones from several genera similar to that of modern warm-blooded mammals (e.g., Ayliffe et al., 1994; Stephan, 1999) and below that of extant ectotherms

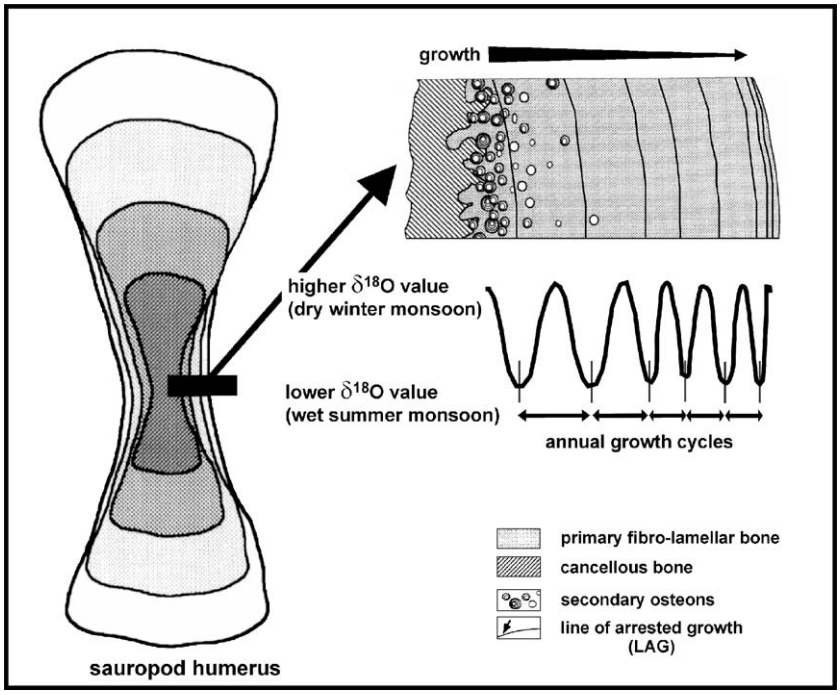

Fig. 3. Schematic cross section of a sauropod humerus and the histology of the primary fibrolamellar bone with multiple LAGs modified after Sander (1999). Possible correlation of LAGs with potential annual climate seasonality recorded in oxygen isotope composition of primary bone phosphate along the axis of radial bone growth. The scale of the $\delta^{18}O$ values is arbitrary. The seasonal variation of the oxygen isotope composition can potentially be used as an annual time marker in skeletochronology to independently confirm the annual nature of LAGs as growth marks. Note that a LAG is a hiatus of unknown duration, during which no bone tissue is deposited, thus part of the seasonal isotopic record can be missing, potentially biasing the seasonal amplitude of $\delta^{18}O$ values. Sinusoidal curves of $\delta^{18}O$ values are thus oversimplified.

(Barrick et al., 1997; Stoskopf et al., 2001) suggest homeothermy and a high metabolic rate for some dinosaur species (Barrick and Showers, 1994; Barrick et al., 1996, 1997; Showers et al., 2002). Also the pattern of $\delta^{18}O_p$ difference between sympatric theropod dinosaurs and ectotherm crocodilians along a latitudinal temperature gradient (Fricke and Rogers, 2000) corroborates this finding. If homeothermy is assumed for large sauropods analyzed in this study, this variation of oxygen isotope composition of the biogenic apatite within skeletal elements should reflect the external seasonal variation of ingested meteoric water like for mammals (Longinelli, 1984; Luz and Kolodny, 1985). In poikilothermic vertebrates, oxygen isotope compositions record a combination of changing body temperature and isotopic composition of ingested water. In both cases, seasonal variations of $\delta^{18}O_p$ values along the radial direction of growth would be recorded in the primary dinosaur bone tissue (Fig. 3). These are expected to be more pronounced for a poikilothermic dinosaur with larger body temperature variations and less pronounced for an endothermic or mass homeothermic dinosaur with a constant body temperature.

1.3. Geologic setting of the Junggar Basin

The geographic position of the Junggar Basin, Xinjiang Province, NW China, is at ~45°N latitude today (Fig. 4), nearly the same paleolatitude as during the Jurassic (Scotese, 2001). The Junggar Basin is a large continental sedimentary basin covering an area of 13,000 km^2 and is filled with a continuous up to 16-km-thick sedimentary succession of terrestrial sediments from the Permian to the Upper Cretaceous (e.g., Zhiyi and Dean, 1996; Tang et al., 1997). The basin fill of the Junggar Basin contains an up to 6-km-thick sedimentary succession

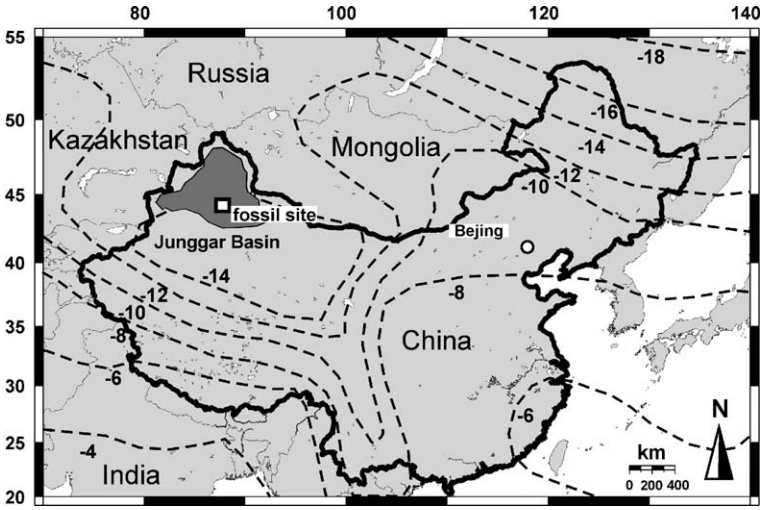

Fig. 4. Map of the Junggar Basin (dark grey) in NW China. The location north of Jiangjunmiao where the dinosaur fossils were found is marked (□). Stippled lines are isolines of mean $\delta^{18}O_{H2O}$ values in water of modern precipitation of China after data from Rozanski et al. (1993). The numbers are the $\delta^{18}O_{H2O}$ values in per mil.

of fluviatile to lacustrine Mesozoic sediments with several fossil sites rich in well-preserved Mesozoic vertebrate remains and fossil woods (Zhao, 1980; McKnight et al., 1990; Dong, 1992; Wang et al., 2000). Often the Mesozoic strata are covered by up to 4-km-thick Cenozoic clastic sediments while in the study area north of Qitai, by this is not the case. The stratigraphy, sedimentology, palynology and coal petrography of these partly coal- and fossil-bearing sediments has been studied in detail (Zhao, 1980; Regional Stratigraphy of Xinjiang, 1981; McKnight et al., 1990; Hendrix et al., 1992). The greenish mud- and siltstones as well as red, fine-grained sandstones of the Upper Jurassic Shishugou Formation contain many well-preserved fossil vertebrate remains from a rich Late Jurassic vertebrate fauna. Different dinosaur genera are known from the fossil record, large sauropods, including *Mamenchisaurus sinocanadorum*, medium sized theropods, *Sinraptor dongi*, and small ornithopods such as *Gongbusaurus wucaiwanensis* (Dong, 1989, 1992; Currie and Zhao, 1993; Russell and Zheng, 1993). Additionally, crocodiles, turtles, lizards, nonmammalian synapsids and small primitive mammals (Triconodonta) are found. Macro-floral remains in the form of silicified fossil woods and even whole petrified forests (McKnight et al., 1990; Wang et al., 2000) are abundant in the Shishugou formation (“Shishu” means “stone tree” in Chinese language).

The paleoclimate in central Asia changed from more humid conditions in Early and Middle Jurassic towards more dry and seasonal climate conditions in the Late Jurassic (McKnight et al., 1990; Keller and Hendrix, 1997). A strong climate seasonality with shortage of water as the main factor limiting growth during the winter dry season is also supported by distinct growth rings in fossil conifer wood samples from contemporaneous Late Jurassic petrified forests (Keller and Hendrix, 1997; Wang et al., 2000; Pfretzschner et al., 2001). This setting with well-preserved vertebrate remains and fossil forests bears the rare chance to study a relatively complete Jurassic ecosystem and the effects of a seasonal Mesozoic megamonsoon paleoclimate (Parrish et al., 1982; Kutzbach and Gallimore, 1989; Vakrhameev, 1991) with annual cyclicity in rainfall (Loope et al., 2001) on the flora and fauna.

2. Material and methods

The fossil dinosaur bones analyzed in this study were collected in the Junggar Basin during field work of the Geologic Institute Tübingen in 1999 and 2000,

in Qitai County, 35 km north of Jiangjunmiao (Fig. 4), as part of an ongoing Chinese-German scientific cooperation program. The bones were found in the upper part of the Upper Jurassic Shishugou Formation in a 72-m-thick section of fluvial limnic sandstones with a few intercalated siltstones and conglomerates (Pfretzschner et al., 2001). The vertebrate fossil bearing strata consist mainly of cross-bedded, fine-grained red sandstones overlain by greenish siltstones and fine sands with iron staining. Identification of the dinosaur species as well as the exact type of bone has not been possible due to the fragmented nature of the specimens.

2.1. Bone specimens

Several bone fragments of primary compact dinosaur bone from the Jurassic Shishugou Formation of the Junggar Basin were investigated for their histology and oxygen isotopic composition. These bone specimens probably belong to different sympatric individuals from the same stratigraphic level of the Shishugou Formation as they were found scattered on the erosional surface of the bone bearing sediment strata (Pfretzschner et al., 2001). The fibrolamellar bones displaying multiple LAGs (Figs. 1a and 2) belonged to a sauropod skeleton from which parts of the pelvis and a fragment of a femur were visible at the sediment surface. Identification of the species has not been possible due to the fragmented nature of the specimens but the fibrolamellar bone (Fig. 1a) investigated in detail (Figs. 5 and 6) probably belongs to the pelvic girdle. The fragment of the thick compacta of plexiform dinosaur bone (Fig. 1b) was found several hundred meters away from the location of the partial sauropod skeleton were the other fragments of fibrolamellar bone were found. Due to the thickness of the compacta (3 cm) and the histology, this bone probably belonged to a large sauropod though an attribution to a large theropod or hadrosaurid

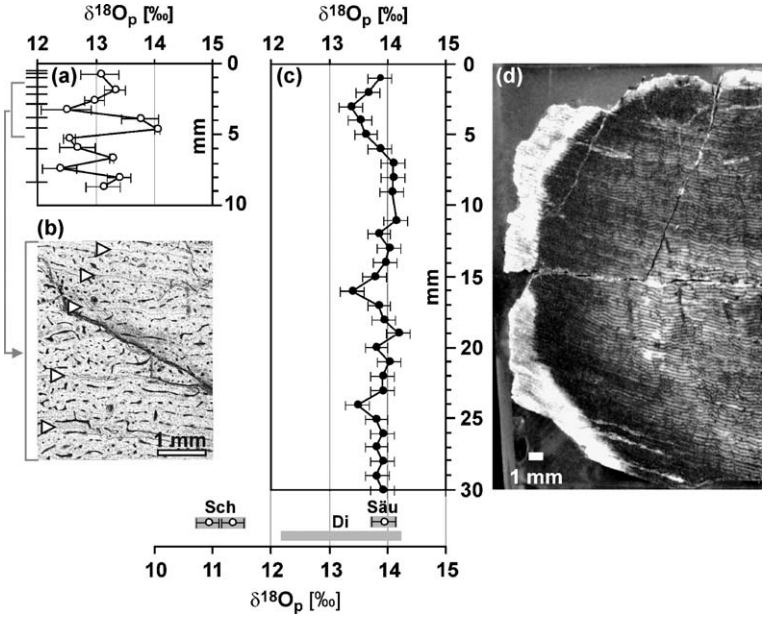

Fig. 5. High-resolution profiles of the oxygen isotopic composition of bone phosphate ($\delta^{18}O_p$) of the two compact dinosaur bones with different histology. (a) $\delta^{18}O_p$-values of the 9-mm-thick fibrolamellar, discontinuous grown dinosaur bone with multiple LAGs (—). (b) Photomicrograph of a detail from the fibrolamellar compacta with five LAGs (white triangles). (c) $\delta^{18}O_p$-profile of the 30-mm-thick plexiform, continuously grown sauropod without any LAGs. (d) Photo of the cross section of the plexiform sauropod bone, the dark color is due to diagenetic manganese-oxides and the white-colored rim is bleached. For comparison the $\delta^{18}O_p$-values of two turtle bones (Sch), a nonmammalian synapsid (Säu): *Bienotheroides ultibmus*, as well as the range of $\delta^{18}O_p$-values from other dinosaur bones ($n=4$) from the same locality (Di) are also shown. Error bars are 1σ for (a) and analytical error for (c).

cannot be excluded (Sander, personal communication, 2003).

Thin sections of the dinosaur bones were prepared and the histology was investigated with transmitted light microscopy to identify growth structures such as LAGs or variations in the density of vascularization. Multiple LAGs (6 to 27) in fibrolamellar bone indicating a periodic (bone) growth were a common feature of several bone specimens (Figs. 1a and 2a), but also a specimen of plexiform bone without any LAGs indicating a continuous (bone) growth was found (Fig. 1b). For one specimen of each type of primary bone tissue, a high-resolution profile of the oxygen isotopic composition of the bone phosphate was analyzed (Fig. 5) to reveal if seasonal climatic variations are responsible for the different histologic growth patterns of the dinosaur bones and the formation of LAGs.

As in the Junggar Basin the strong annual seasonality of a monsoon-type climate is reflected in fossil wood from contemporary deposits (Keller and Hendrix, 1997; Wang et al., 2000), it may have been the cause for the formation of LAGs in fibrolamellar dinosaur bone. To test this hypothesis and the annual nature of the LAGs a dinosaur bone fragment with multiple LAGs in fibrolamellar bone was investigated in detail with histological and geochemical methods (Fig. 6). The investigated specimen of fibrolamellar bone is a platy bone fragment with a 9-mm-thick compacta in the direction of radial growth. It has 10 identifiable LAGs, of which 7 belong to the fibrolamellar part and 3 to the outer lamello-zonal bone (Fig. 6). The presence of the external lamellar-zonal system combined with the fact that the primary bone compacta contains none or only very few isolated secondary osteons points towards a specimen from a young adult without significant bone remodeling and preservation of primary histological growth structures. For comparison purposes, a 30-mm-thick piece of compact, plexiform bone specimen without any features of

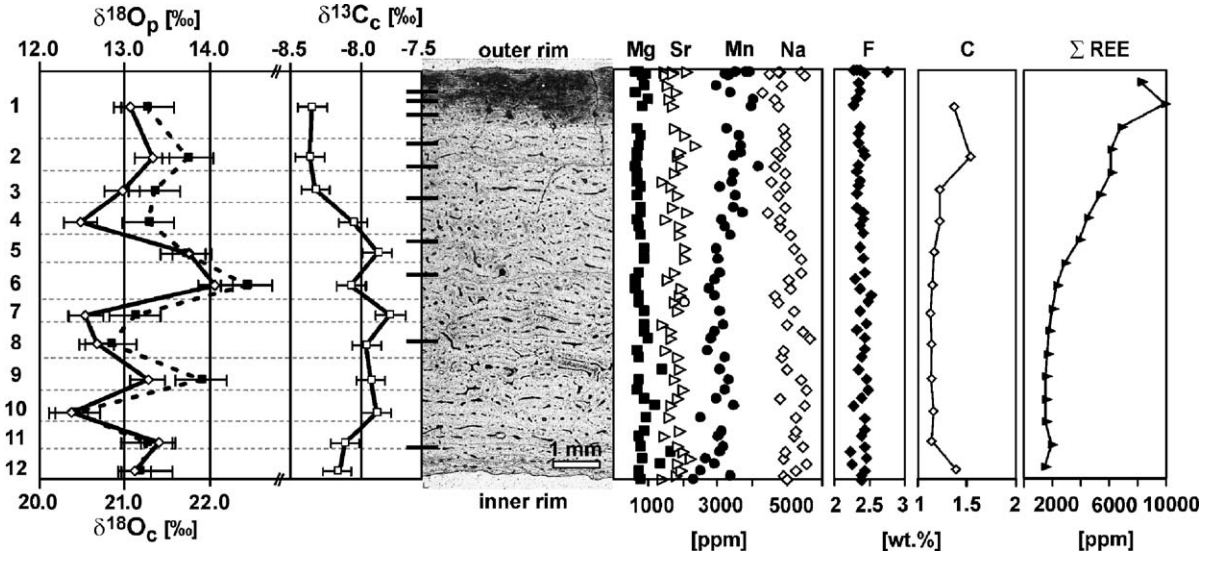

Fig. 6. Photomicrograph of a complete cross section of the fibrolamellar sauropod bone investigated for oxygen and carbon isotopic as well as elemental composition. The primary bone histology of fibrolamellar type is well preserved without any traces of remodeling and the compacta contains at least identifiable 10 LAGs (—). Boundaries of the intervals sampled for isotopic measurements (▪▪▪). Numbers at the left edge of the diagram are sample numbers from Table 1. $\delta^{18}O_c$ (■) and $\delta^{18}O_P$ (◇) values over the profile indicate changes of the oxygen isotopic composition of the body water during bone formation are still preserved. The bone intervals with LAGs often have higher $\delta^{18}O$ values while samples with no LAGs have the lowest values. $\delta^{13}C_c$ values of the carbonate in the phosphate (□) vary only slightly around −8.1‰. Error bars of $\delta^{18}O$ and $\delta^{13}C_c$ values are analytical errors. Most trace elements (Mg, Sr, Mn, Na) as well as the major elements (Ca, P, F) are relatively homogenously distributed throughout the bone profile and do not indicate any cyclic pattern or anomalies around the LAGs as observed for the $\delta^{18}O_c$ and $\delta^{18}O_P$ values. Only REE and carbon concentrations are diagenetically enriched towards the bone rims.

remodeling and no LAGs (Fig. 1b), indicating a continuous growth, was also investigated. Due to its origin from a partially articulated skeleton, its thick compacta and bone histology, this specimen probably belonged to a large sauropod.

The bone fragments were embedded in epoxy resin and a cube was cut using a diamond micro-saw. From the cross section of the cube samples of bone powder were scraped off parallel to bone growth layers in sub-mm to mm intervals from the outer cortex towards the marrow cavity with a Proxxon Mini-drill. From the fibrolamellar bone with multiple LAGs a complete profile of 12 samples in sub-mm resolution was scraped off perpendicular to the radial direction of growth, sampling areas with and without LAGs (Fig. 6). From the plexiform bone a profile of 30 samples at 1 mm increments was sampled. Sub-mm sampling is necessary to get temporal resolution of annual seasonality in the stable isotope composition of bone phosphate as bone apposition rates are calculated to be 1.7 to 3.9 mm/year for compact sauropod bone (Sander and Tückmantel, 2003).

2.2. Analytical methods

After a two-step chemical cleaning procedure with 2.5% NaOCl and 0.125 m NaOH to remove potential organic contaminants, the bone powder was dissolved in 2 m HF. After neutralization of the eluate with 2 m KOH, the PO_4^{3-} was precipitated as silver phosphate (Ag_3PO_4) by addition of ammoniacal silver nitrate solution according to the method of O'Neil et al. (1994) modified by Stephan (2000). The Ag_3PO_4 was fluorinated with BrF_5 at 500 °C in nickel vessels on a conventional extraction line (Vennemann et al., 2002). The O_2 produced (100% yield) was converted with graphite to CO_2. For isotopic analyses of carbonate in phosphate, samples were pretreated with 2.5% NaOCl and a solution of 1 M acetic acid buffered with Ca-acetate (pH 4.5) to remove organic contaminants and diagenetic carbonates, respectively (Koch et al., 1997). The structural CO_3^{2-} in bone phosphate was extracted as CO_2 in an He-carrier gas stream using a Finnigan MAT GasBench II, reacting 1 mg of rinsed and dried pretreated sample powder for 27 h at 70 °C with 100% orthophosphoric acid. The resultant CO_2 of both procedures was measured for its oxygen isotope composition of phosphate ($\delta^{18}O_p$) and the oxygen and carbon isotope composition of carbonate ($\delta^{18}O_c$, $\delta^{13}C_c$) using a Finnigan MAT 252 isotope ratio mass spectrometer. The oxygen and carbon isotope results are reported in the conventional δ-notations in per mil deviations from VSMOW and VPDB standard, respectively. ($\delta_{sample}=[(R_{sample}-R_{standard})/R_{standard}]\times 1000$; with $R=^{18}O/^{16}O$ and $^{13}C/^{12}C$, respectively; $\delta=\delta^{18}O$ and $\delta^{13}C$, respectively). $\delta^{18}O_p$ was determined in duplicate or triplicate for the fibrolamellar bone (Table 1). The internal labora-

Table 1
Carbon and oxygen isotope data of the fibrolamellar bone profile

Sample	Bone type	Profile (mm)	$\delta^{18}O_p$ [a] (‰)	LAG	S.D.	n	$\delta^{18}O_c$ [a] (‰)	$\delta^{13}C_c$ [b] (‰)	$\Delta(\delta^{18}O_c-\delta^{18}O_p)$ (‰)	C (wt.%)
FK DI JU 12 (1)	fibrolamellar	0.8	13.1	Yes	0.3	3	21.3	−8.3	8.2	1.4
FK DI JU 12 (2)	fibrolamellar	1.9	13.3	Yes	0.2	3	21.7	−8.4	8.4	1.5
FK DI JU 12 (3)	fibrolamellar	2.6	13.0	Yes	0.2	2	21.4	−8.3	8.4	1.2
FK DI JU 12 (4)	fibrolamellar	3.3	12.5	No	0.4	3	21.3	−8.1	8.8	1.2
FK DI JU 12 (5)	fibrolamellar	3.9	13.8	Yes	0.3	3	21.7	−7.9	8.0	1.2
FK DI JU 12 (6)	fibrolamellar	4.6	14.1	Yes	0.0	2	22.4	−8.1	8.4	1.1
FK DI JU 12 (7)	fibrolamellar	5.3	12.5	No	0.1	2	21.1	−7.8	8.6	1.1
FK DI JU 12 (8)	fibrolamellar	5.9	12.7	Yes	0.3	2	20.8	−8.0	8.2	1.1
FK DI JU 12 (9)	fibrolamellar	6.7	13.3	Yes	0.0	2	21.9	−7.9	8.6	1.1
FK DI JU 12 (10)	fibrolamellar	7.4	12.4	No	0.3	2	20.4	−7.9	8.0	1.2
FK DI JU 12 (11)	fibrolamellar	8.0	13.4	Yes	0.2	2	21.3	−8.1	7.9	1.1
FK DI JU 12 (12)	fibrolamellar	8.6	13.1	No	0.3	2	21.3	−8.1	8.1	1.4
Mean			13.1				21.4	−8.1	8.3	1.2
S.D.			0.5				0.5	0.2	0.3	0.1

[a] Oxygen isotopic composition of bone phosphate ($\delta^{18}O_p$) and carbonate in phosphate ($\delta^{18}O_c$) relative to VSMOW.
[b] Carbon isotopic composition ($\delta^{13}C_c$) relative to VPDB.

tory standards GW-1 (great white shark tooth phosphate) and HAP (synthetic hydroxy apatite) gave an analytical precision of 0.2 ‰ (1σ) for $\delta^{18}O_p$ and $\delta^{18}O_c$ and 0.1 ‰ (1σ) for $\delta^{13}C_c$. Electron microprobe analyses (EMPA) of major (Ca, P) and trace element (Sr, Mg, Na, S, Fe, Mn, Si, F and Cl) composition were performed with a JXA 8900 RL JEOL electron microprobe on polished and carbon coated thin sections. Element concentrations were measured as quantitative single points in the wavelength dispersive (WDS) mode along a transect across the bone compacta under vacuum conditions of $< 10^{-5}$ mbar with 15 kV high voltage, 15 nA beam current, using a 10 μm defocussed electron beam.

The rare earth element composition was analyzed using laser inductive coupled plasma time of flight mass-spectrometry (LA-ICP-TOF-MS) with an argon-fluoride excimer laser COMPex™ 110 with $\lambda = 193$ nm from Lambda Physik® in combination with the optical bank GeoLas 100 Q from MicroLas Lasersystem. Material was ablated in 100 μm spots and measured in an LECO Renaissance™ ICP-TOF-MS. Details for both EMPA and LA-ICP-MS in situ microanalyses procedures are given in Tütken (2003).

3. Results

The two bone specimens of the dinosaurs differ in their bone histology (Fig. 1) and bone layer thickness (see Fig. 1 for detailed explanations). One bone is of fibrolamellar type displaying multiple LAGs representing periods of interrupted bone growth (Fig. 1a) and has an average bone layer thickness of 209 μm (S.D. = 44, $n = 36$) (Fig. 7a). The other bone is of plexiform type (Fig. 1b) indicating a continuous bone growth at a similar rate and has an average bone layer thickness of 247 μm (S.D. = 25, $n = 106$) (Fig. 7b).

Measurements of the thickness of the bone layers between the vascular layers in the fibrolamellar bone yield cyclic variations, which correspond to the position of the LAGs (Fig. 7a). Each cycle begins with the deposition of bone layers of about 250 μm thickness. The last two or three layers formed before the LAG are considerably thinner (about 150 μm) and each cycle ends with a LAG (Fig. 7a). The reduced spacing of the LAGs towards the outer cortex in the specimen with multiple LAGs (Fig. 7a) indicates a periodic cessation of bone growth and a simultaneous decrease in overall growth rate. In contrast, the plexiform bone

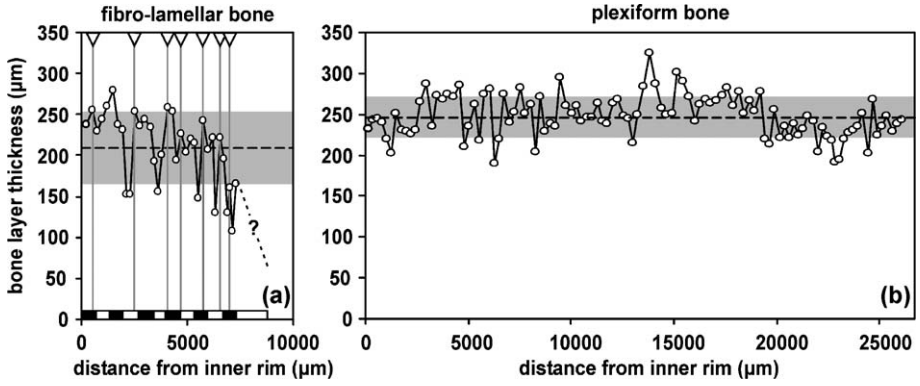

Fig. 7. The plot shows the thickness (μm) of successive bone layers between two adjacent vascular layers in the fibrolamellar and plexiform sauropod bone specimens. The average bone layer thickness (▪▪▪) and its standard deviation (▮) are given. (a) The bone layer thickness in the fibrolamellar sauropod bone with multiple LAGs displays cyclicity. Each cycle begins with the deposition of thick bone layers (~ 250 μm) followed by a few thin layers (~ 200 to 150 μm) and closes with a LAG. The positions of LAGs are indicated by grey vertical lines. As each LAG is positioned in a bone layer (definition of a bone layer is given in Fig. 1), the LAGs appear always in the first thick layer in the plot. The layers that contain a LAG represent two distinct phases of bone deposition, one before and one after the pause during which the LAG was formed. In the poorly vascularized lamello-zonal bone that forms the outer ~ 1.5 mm bone layers deposited during the adult stage were not distinguishable (▪ ? ▪) due to the reduced rate of bone growth. Intervals sampled for isotopic analyses are marked by alternating black and white bars. (b) The bone layer thickness of the plexiform sauropod bone without LAGs displays continuous bone growth with greater average bone layer thickness and smaller standard deviation compared to the fibrolamellar sauropod bone.

Table 2
Oxygen isotope data of the bone phosphate of the plexiform bone profile

Sample	Bone type	Profile (mm)	$\delta^{18}O_p$ (‰)
FK DI JU 13 (1)	plexiform	1	13.9
FK DI JU 13 (2)	plexiform	2	13.7
FK DI JU 13 (3)	plexiform	3	13.4
FK DI JU 13 (4)	plexiform	4	13.6
FK DI JU 13 (5)	plexiform	5	13.7
FK DI JU 13 (6)	plexiform	6	13.9
FK DI JU 13 (7)	plexiform	7	14.2
FK DI JU 13 (8)	plexiform	8	14.2
FK DI JU 13 (9)	plexiform	9	14.1
FK DI JU 13 (10)	plexiform	10	n.d.
FK DI JU 13 (11)	plexiform	11	14.2
FK DI JU 13 (12)	plexiform	12	13.9
FK DI JU 13 (13)	plexiform	13	14.1
FK D1 JU 13 (14)	plexiform	14	14.0
FK DI JU 13 (15)	plexiform	15	13.8
FK DI JU 13 (16)	plexiform	16	13.5
FK DI JU 13 (17)	plexiform	17	13.9
FK DI JU 13 (18)	plexiform	18	14.0
FK DI JU 13 (19)	plexiform	19	14.3
FK DI JU 13 (20)	plexiform	20	13.9
FK DI JU 13 (21)	plexiform	21	14.1
FK DI JU 13 (22)	plexiform	22	14.0
FK DI JU 13 (23)	plexiform	23	14.0
FK DI JU 13 (24)	plexiform	24	13.6
FK DI JU 13 (25)	plexiform	25	13.9
FK DI JU 13 (26)	plexiform	26	14.0
FK DI JU 13 (27)	plexiform	27	13.9
FK DI JU 13 (28)	plexiform	28	14.0
FK DI JU 13 (29)	plexiform	29	13.9
FK DI JU 13 (30)	plexiform	30	14.0
Mean			13.9
S.D.			0.2

n.d. = not determined; due to sample loss during preparation.

has bone layers of more constant thickness of around 250 μm throughout the profile (Fig. 7b). A Fourier analysis, which is a time series analysis on the basis of the Fourier transformation, was applied to the sequence of measurements of the bone layer thickness to detect a possible cyclicity. In this method, the series of measurements is described as a sum of sinus- or cosinus-functions. If there is any cyclicity in the sequence, the trigonometric functions with the corresponding frequency will show up with a higher amplitude. Such analyses, however, also indicate a weak cyclicity in the plexiform bone similar to that in the fibrolamellar bone with LAGs (Pfretzschner et al., 2001).

The differences in bone histology are also reflected in the oxygen isotope composition of the two specimens (Fig. 6). The fibrolamellar bone with multiple LAGs and cycles in bone layer thickness (Fig. 7a) has mean $\delta^{18}O_p$ and $\delta^{18}O_c$ values of 13.2‰ (S.D. = 0.5, $n = 12$) and 21.4‰ (S.D. = 0.5, $n = 12$) and an intra-bone variability of 1.7‰ and 2.1‰, respectively (Fig. 6, Table 1). Furthermore, a *t*-test of the means of the $\delta^{18}O_p$ values yields significantly ($\alpha = 0.05$) higher values for bone samples that contain one or more LAGs (average $\delta^{18}O_p = 13.34$‰, S.D. = 0.44, $n = 7$) compared to those for samples of samples without any LAG (average $\delta^{18}O_p = 12.63$‰, S.D. = 0.32, $n = 4$). The plexiform bone has a higher mean $\delta^{18}O_p$ value of 13.9‰ (S.D. = 0.2, $n = 30$) and a smaller intra-bone variability for $\delta^{18}O_p$ values of ≤ 0.8‰ (Fig. 5, Table 2).

The $\delta^{18}O_p$ intra-bone variation of the fibrolamellar bone specimen is in the range of the annual intra-tooth variation of $\delta^{18}O_p$ values measured on modern and fossil high-crowned mammal teeth (Bryant et al., 1996a; Sharp and Cerling, 1998) but is smaller than that observed in modern and fossil bones and teeth of ectotherm crocodiles (Barrick et al., 2001; Stoskopf et al., 2001). The range of $\delta^{18}O_p$ values is similar to those measured on four sympatric dinosaur bone samples (12.1‰ to 14.1‰) and one small tritylodontid *Bienotheroides ultibmus* (13.8‰), but is 2‰ higher than that of turtle bones (11.2‰, S.D. = 0.2, $n = 2$) (Fig. 5, Table 3).

The variation of $\delta^{18}O_p$ and $\delta^{18}O_c$ values in the fibrolamellar bone has a cyclic pattern (Fig. 6). Samples from increments between the LAGs (sample 4, 7, 10 and 12) do display the lowest $\delta^{18}O$ values resulting in distinct minima of the intra-bone variation of $\delta^{18}O$ values (Fig. 6), the only exception is sample 9. In contrast, samples from increments that contain

Table 3
Oxygen isotope data of dinosaur and turtle bones

Sample	Type	$\delta^{18}O_p$ (‰)
FK DI JU 8	dinosaur	13.7
FK DI JU 11	dinosaur	13.9
FK DI JU 6	dinosaur	12.1
FK DI JU 10	dinosaur	14.1
FK BIE JU 1	reptile	13.8
FK SCH JU 1	turtle	10.9
FK SCH JU 5	turtle	11.4

LAGs (sample 1, 2, 3, 5, 6 and 11) generally display $\delta^{18}O_p$ values that are on average 0.7‰ higher than increments without LAGs (Fig. 6) and coincide with the maxima of the intra-bone variation of $\delta^{18}O$ values (sample 5, 6, 11), except for sample 8. In contrast, carbon isotope compositions ($\delta^{13}C_c$) vary only slightly from −7.9‰ to −8.4‰ throughout the whole profile with an average value of 8.1‰ (S.D. = 0.2, $n = 12$) (Fig. 6).

In situ investigations of the chemical composition and XRD investigations of apatite crystallinity indicate complete recrystallization of the biogenic apatite of the bone compacta to a homogeneous carbonate-fluorapatite with average F contents of about 2.4 wt.% (Table 4, Fig. 6). Average REE contents of ~2400 ppm in the fibrolamellar bone (Table 5) also indicate a strong diagenetic REE enrichment of four orders of magnitude compared to very low REE contents in fresh mammal bones (320 ppb, S.D. = 180, $n = 12$; Tütken, 2003). REE contents are also higher than in most Cenozoic fossil mammal bones (~100 ppb to 1930 ppm, $n = 91$; Tütken, 2003). Furthermore, REE concentrations display an up to five-fold increase towards the outer rim (Table 5; Fig. 6). Besides the REEs, the carbon content in the rims is enriched compared to the average value for the fibrolamellar bone (Fig. 6). The other major and trace elements are homogeneously distributed in the profile and do not

Table 4
In situ electron microprobe major and trace element data (in wt.%) of the fibrolamellar dinosaur bone profile

µm	CaO	P_2O_5	MgO	FeO	Na_2O	SrO	MnO	SiO_2	F	Cl	Total
85	47.67	34.88	0.09	3.23	0.59	0.19	0.37	0.32	2.53	0.06	90.42
170	46.30	33.48	0.10	6.09	0.56	0.22	0.35	0.49	2.21	0.05	90.31
383	46.50	36.09	0.10	1.13	0.56	0.24	0.44	0.17	2.39	0.05	88.15
510	43.31	35.85	0.13	0.15	0.64	0.23	0.42	0.19	2.50	0.06	83.85
680	48.58	36.12	0.11	0.24	0.61	0.19	0.40	0.20	2.33	0.07	89.24
1020	48.88	36.27	0.11	0.42	0.64	0.25	0.41	0.24	2.39	0.06	90.09
1190	44.51	36.20	0.11	0.62	0.62	0.19	0.46	0.12	2.23	0.06	85.51
1424	46.08	35.22	0.24	0.71	0.65	0.21	0.50	2.03	2.24	0.06	88.25
1721	39.89	35.58	0.09	0.07	0.62	0.22	0.44	0.15	2.31	0.07	79.77
1934	50.34	35.62	0.14	0.22	0.66	0.24	0.38	0.20	2.44	0.08	90.57
2189	49.31	35.99	0.13	0.13	0.66	0.21	0.48	0.17	2.42	0.06	89.84
2593	50.55	35.79	0.12	0.08	0.66	0.22	0.38	0.06	2.45	0.06	90.69
2975	49.86	35.48	0.12	0.10	0.66	0.21	0.37	0.06	2.41	0.08	89.52
3273	50.31	37.06	0.10	0.12	0.63	0.18	0.36	0.07	2.35	0.08	91.82
3549	49.52	35.10	0.08	0.10	0.70	0.22	0.26	0.03	2.50	0.08	88.82
3868	50.81	36.27	0.05	0.09	0.67	0.20	0.28	0.06	2.49	0.08	91.19
4123	50.14	36.56	0.09	0.11	0.70	0.21	0.29	0.03	2.50	0.07	90.87
4378	50.83	36.03	0.10	0.10	0.64	0.20	0.25	0.07	2.51	0.06	90.88
5355	50.66	35.95	0.11	0.19	0.58	0.15	0.30	0.19	2.38	0.09	90.89
5865	51.08	36.27	0.08	0.13	0.68	0.16	0.25	u.d.	2.62	0.08	91.47
6141	50.95	35.79	0.11	0.06	0.66	0.17	0.29	0.04	2.46	0.09	90.68
6715	50.83	36.03	0.09	0.07	0.65	0.18	0.28	0.10	2.38	0.10	90.83
7098	50.48	36.09	0.11	0.13	0.69	0.22	0.30	0.16	2.44	0.10	90.87
7416	50.44	35.89	0.09	0.10	0.75	0.24	0.23	0.09	2.46	0.10	90.53
7735	50.52	37.07	0.10	0.13	0.76	0.13	0.26	u.d.	2.51	0.10	91.74
7990	49.06	34.47	0.19	0.32	0.68	0.20	0.34	1.48	2.27	0.10	89.22
8670	50.29	35.76	0.11	0.10	0.68	0.15	0.24	0.09	2.52	0.08	90.08
9053	49.66	36.34	0.09	0.10	0.62	0.19	0.23	u.d.	2.53	0.10	90.00
9435	49.63	36.97	0.08	0.15	0.62	0.17	0.30	0.09	2.46	0.08	90.63
9733	49.06	35.79	0.09	0.09	0.70	0.20	0.26	0.07	2.42	0.06	88.90
10115	49.99	36.99	0.10	0.08	0.70	0.18	0.16	0.01	2.38	0.09	90.84
mean	48.90	35.90	0.11	0.50	0.65	0.20	0.33	0.25	2.42	0.07	89.56
S.D.	2.57	0.75	0.03	1.19	0.05	0.03	0.09	0.44	0.10	0.02	2.48

u.d. = under the detection limit of the electron microprobe.

Table 5
REE concentrations (ppm) of in situ LA-ICP-MS measurements of the fibrolamellar bone profile

Sample point	La	Ce	Pr	Nd	Sm	Eu	Gd	Tb	Dy	Ho	Er	Tm	Yb	Lu	ΣREE
FK DI JU 12 (1)	2069	2510	538	2165	430	60	327	38	176	34	81	11	55	8	8500
FK DI JU 12 (2)	2247	3708	634	2265	494	67	349	41	189	35	83	10	53	7	10,181
FK DI JU 12 (3)	1916	2047	443	1702	322	47	267	30	144	28	69	9	46	6	7076
FK DI JU 12 (4)	1840	1824	377	1449	267	40	238	27	130	26	64	9	44	6	6341
FK DI JU 12 (5)	1956	1729	362	1382	246	38	233	27	139	30	77	10	52	7	6289
FK DI JU 12 (6)	1821	1533	311	1169	207	34	210	24	129	29	76	10	53	7	5613
FK DI JU 12 (7)	1664	1255	229	847	144	25	162	19	102	23	63	9	45	6	4594
FK DI JU 12 (8)	1436	1258	174	623	105	19	128	14	82	20	55	8	41	6	3968
FK DI JU 12 (9)	1265	698	135	491	78	15	107	12	72	18	51	7	39	6	2993
FK DI JU 12 (10)	1022	597	98	354	55	11	84	9	57	15	44	6	36	5	2394
FK DI JU 12 (11)	960	403	83	303	47	9	76	8	53	14	43	7	36	5	2048
FK DI JU 12 (12)	867	365	69	247	38	8	67	7	47	13	40	6	34	5	1814
FK DI JU 12 (13)	880	231	67	245	37	8	66	7	48	13	42	6	35	5	1691
FK DI JU 12 (14)	797	256	60	217	34	7	61	7	44	12	38	6	33	5	1576
FK DI JU 12 (15)	808	248	62	225	34	7	63	7	44	12	38	6	33	5	1592
FK DI JU 12 (16)	799	250	65	233	36	7	64	7	44	12	37	6	32	5	1596
FK DI JU 12 (17)	889	477	78	278	45	9	73	8	50	13	40	6	34	5	2004
Mean	1022	597	98	354	55	11	84	9	57	15	44	6	36	5	2394

show any cyclic variation as observed for the $\delta^{18}O$ values (Fig. 6).

4. Discussion

Both sauropod bone fragments (the fibrolamellar bone as well as the plexiform bone) have not experienced significant in vivo bone remodeling of the primary bone tissues as indicated by the lack of secondary osteons (Fig. 1). The plexiform bone specimen with a 30-mm-thick compacta (Fig. 5d) indicates a continuous growth of 8 to 18 years calculated on the basis of deposition rates for compact bones of sauropods of 1.7 to 3.9 mm/year (Sander and Tückmantel, 2003). In contrast, the fibrolamellar bone fragment with 10 LAGs (Fig. 6) grew discontinuously with much slower growth rates of 2.3 to <0.5 mm/year over a minimum period of 10 years (assuming annual formation of LAGs). In accordance with the ontogenetic bone histology of the sauropod Apatosaurus (Curry, 1999), a decrease in growth rate towards the end of the main ontogenetic growth as indicated by the formation of LAGs in fibrolamellar bone, decreasing distance between the LAGs in direction of growth (Fig. 1a), and the deposition of lamello-zonal bone at the outer rim of this specimen can be inferred. The fibrolamellar bone fragment with 27 LAGs (Fig. 2) that probably belongs to the pelvic girdle of the same partial sauropod skeleton of the sub-adult to adult individual from which the bone specimen with 10 LAGs originates would, however, give a biological age estimate of at least 27 years. Because deposition patterns of bone tissue depend on various phylogenetic, functional, and biomechanical factors (e.g., de Ricqlès et al., 1991) bone histology and the abundance of growth marks like LAGs can differ significantly between different bones from an individual dinosaur and even within a single skeletal element due to asynchronous bone deposition (Curry, 1999; Horner et al., 2000). The large number of LAGs observed for the pelvic bone fragment is in accordance with the observation of abundant LAGs in sauropod pelvic elements (Reid, 1981). The estimated age range for this individual sauropod of unknown species based on the LAGs range from a minimum age of 10 to 27 years indicative of sub-adult to adult ages compared to Apatosaurus growth rates reaching the sub-adult stage within 8 to 10 years (Curry, 1999). Such differences in growth mark abundances within individual dinosaurs are a severe problem for estimates of biological ages and hence an inference of overall growth rates.

A seasonal variation of the oxygen isotopic composition of bone phosphate that may be preserved in fast-growing primary bone tissue without significant

in vivo remodeling would potentially allow for an inference to the season of bone deposition. This opens up the possibility of an independent age estimate and provides a time frame for the formation of growth marks and hence improve the skeletochronology and growth rate estimates.

Oxygen is principally located in the phosphate and carbonate groups of bone apatite, both of which are precipitated in equilibrium with body fluids. Hence, the $\delta^{18}O_c$ and $\delta^{18}O_p$ values in modern vertebrate skeletal remains are positively correlated, with observed fractionations of between 8.4 ‰ and 9.0 ‰ (e.g., Bryant et al., 1996b; Iacumin et al., 1996; Fig. 8). Because of different rates of isotopic exchange between carbonate-water and phosphate-water, Iacumin et al. (1996) have noted that $\delta^{18}O_c$ and $\delta^{18}O_p$ values of altered bone samples can deviate from a line of constant isotopic fractionation between carbonate and phosphate, with $\delta^{18}O_c$ values being more susceptible to change. However, once both oxygen in carbonate within phosphate and oxygen from phosphate have experienced complete diagenetic exchange, the $\delta^{18}O_c$ and $\delta^{18}O_p$ values can again plot on a line of constant isotopic fractionation but at the same time original heterogeneities in values will tend to be homogenized.

The preservation of pristine oxygen isotope compositions is a prerequisite for all interpretations of paleoclimate and/or paleobiology on the basis of $\delta^{18}O_p$ and $\delta^{18}O_c$ values of fossil biogenic phosphates. Diagenesis is thus a major concern for geochemical analysis of Mesozoic fossil phosphate (Hubert et al., 1996; Kolodny et al., 1996; Elzora et al., 1999). This is especially true for bones, because they are more vulnerable to diagenetic alteration compared to tooth enamel (Nelson et al., 1986; Ayliffe et al., 1994; Kohn et al., 1999; Tütken, 2003), as bone originally consists of very small crystallites that tend to recrystallize to carbonate-fluorapatite (e.g., Lucas and Prevot, 1991; Elzora et al., 1999). Recrystallization in low-temperature sedimentary settings related to microbial PO_4^{3-} degradation (Blake et al., 1997), or exchange of the primary apatite with diagenetic fluids that have distinctly different oxygen isotope compositions compared to original body fluids, or incorporation of secondary diagenetic apatite may all lead to changes in the $\delta^{18}O$ values of the original phosphate (Hubert et al., 1996; Kolodny et al., 1996). While $\delta^{18}O_p$ values of terrestrial bones may be rapidly altered in marine settings (Tütken et al., 2001a; Tütken, 2003), primary oxygen isotopic compositions can be preserved in Mesozoic dinosaur specimens from freshwater settings with an appropriate diagenetic milieu (Barrick et al., 1997; Showers et al., 2002; Tütken, 2003).

Most major and trace elements are homogeneously distributed in the profile and do not show any cyclic variation as observed for the $\delta^{18}O$ values (Fig. 6). Also, the XRD data and REE concentrations of the bones clearly indicate that diagenetic recrystallization of the original biogenic apatite to carbonate-fluorapa-

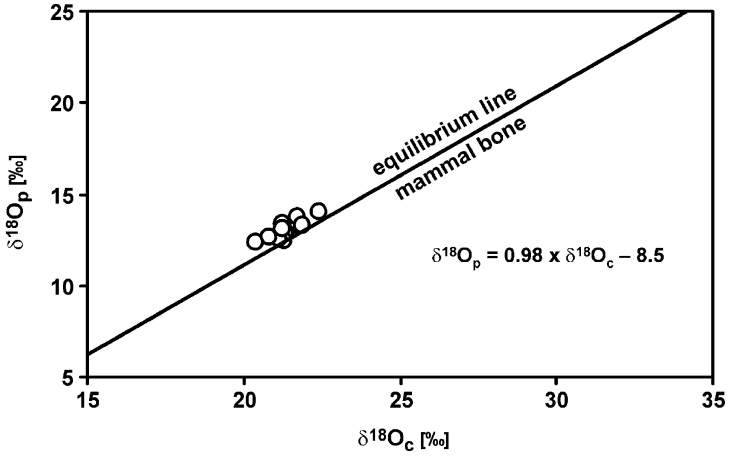

Fig. 8. The dinosaur bone samples plot near the linear relation of $\delta^{18}O_p$ and $\delta^{18}O_c$ established for modern mammals (Iacumin et al., 1996), indicating equilibrium formation of carbonate and phosphate from the same body fluid and thus lack of diagenetic alteration.

tite has occurred and was accompanied by changes in the chemical composition. In Cenozoic fossil mammal bones REE are often enriched up to several orders of magnitude in the outer rim (1 to 2 mm) compared to the central bone compacta (Tütken, 2003). REE gradients were probably fixed in fossil bones after the early diagenetic REE uptake and recrystallization of the bone phosphate to carbonate-fluorapatite. As the REE concentration gradient in this dinosaur bone specimen is not as steep as observed for the fossil mammal bones, possibly a long term, late diagenetic REE incorporation may have occurred.

Because the samples analyzed from the dinosaur bone profile closely follow the linear relation of constant fractionation with average differences between $\delta^{18}O_c$ and $\delta^{18}O_p$ values of 8.3 ‰ (S.D. = 0.3, $n = 12$) (Table 1; Fig. 8) but also preserve a cyclicity in their values, it is apparent that the original $\delta^{18}O$ values have been preserved, despite the recrystallization. Diagenetic alteration affecting major, trace, and REE elements (Fig. 6, see also Trueman and Tuross, 2002) but leaving the oxygen isotope composition unaltered is possible as the lattice sites in apatite for Ca^{2+} and OH^- are more vulnerable to diagenetic exchange processes than the PO_4-site with oxygen being tightly bound to phosphorous in the PO_4-group (c.f. Kohn and Cerling, 2002; Tütken, 2003). A possible mechanism that may allow for preservation of the oxygen isotope compositions is a microscale dissolution–precipitation process that preserves fine histological bone structures (e.g., Zocco and Schwartz, 1994; Trueman and Martill, 2002) and primary $\delta^{18}O$ values.

The cyclic pattern for $\delta^{18}O$ values in the sauropod bone phosphate from the Junggar Basin can thus be interpreted to reflect changes in oxygen isotope composition of the sauropod body fluid during bone growth. The cyclicity of the changes suggests seasonal $\delta^{18}O$ variations. Such seasonal variations are well known from oxygen isotope compositions of modern and fossil phosphate of mammal teeth and tusks (Koch et al., 1989; Bryant et al., 1996a; Fricke and O'Neil, 1996; Kohn et al., 1998; Sharp and Cerling, 1998) as well as reptile and dinosaur teeth (Jensen et al., 1999; Straight et al., 1999; Barrick et al., 2001, Thomas and Carlson, 2001) but have never been reported for bones.

As the fossil fibrolamellar bone has not experienced significant in vivo bone remodeling (lack of secondary osteons) and as diagenetic alteration of the oxygen isotope composition is unlikely, the intra-bone variations in $\delta^{18}O_p$ values can either relate to changes in $\delta^{18}O_{bw}$ and hence ingested meteoric water for homeotherms, or changes in $\delta^{18}O_{bw}$ and/or body temperature for poikilotherms. In both cases, the intra-bone variation of the $\delta^{18}O_p$ values is related to seasonal temperature variations and will potentially allow for the use of histological growth marks (or LAGs) as time markers.

The manual sampling procedure used had a spatial resolution of 0.5 to 1 mm that allowed for 12 samples to be taken of the fibrolamellar bone with 10 LAGs. Unfortunately, individual areas between LAGs and individual LAGs could not be sampled separately in all cases. In some increments, several LAGs were sampled together or only part of a LAG was sampled (Fig. 6). This, together with the relatively small sample number makes it difficult to interpret the statistical meaning of the data. In fact, there is no direct correlation between bone layers with LAGs and the oxygen isotope composition (exact Fisher Test for 2×2 contingency tables with less than five cases yields a significance level of $\alpha = 0.348$). However, a *t*-test indicates a significant difference at $\alpha < 0.05$ between the average oxygen isotope composition of layers containing LAGs with $\delta^{18}O_p = 13.3$ ‰ (S.D. = 0.4, $n = 7$) and layers containing no LAGs with $\delta^{18}O_p = 12.6$ ‰ (S.D. = 0.3, $n = 4$). Because of the large and integrative sampling increments the measured intra-bone variability of 1.7 ‰ and 2.1 ‰ for $\delta^{18}O_p$ and $\delta^{18}O_c$, respectively, is also a minimum estimate only. For a higher sample resolution microsampling devices with a better spatial resolution of < 100 μm and a different method of phosphate analyses (e.g., Showers et al., 2002; Vennemann et al., 2002) would be necessary.

Strong annual seasonality of a Jurassic monsoon-type climate as an exogenous trigger mechanism may explain why the oxygen isotope variations in the fibrolamellar bone generally fits the bone histology and the coincidence between maximum $\delta^{18}O$ values and LAGs. A seasonally evaporitic, semiarid high-pH environment has been indicated by the abundant silicified fossil wood (e.g., Francis, 1984; Wang et al., 2000) and soil horizons as well as chalcedony fillings of bone porosity. Fossilized wood samples from an almost contemporaneous petrified forest of

the lower Shishugou Formation in the Junggar Basin indicate high seasonality and reduced tree growth during the dry season (Wang et al., 2000; Pfretzschner et al., 2001), as was also interpreted to be the case for the Jurassic Prubeck Forest (Francis, 1984). For the Late Jurassic Suihent petrified forest of NE Mongolia thin late wood rings are also interpreted to result from a strong seasonal megamonsoon climate (Keller and Hendrix, 1997) with a seasonally limited water supply during the dry winter responsible for the abrupt end of the growing season. Furthermore, sedimentological studies by McKnight et al. (1990) on the Shishugou Formation that includes the petrified forest and dinosaur bones found bidirectional oriented fossilized trunks and in situ stumps buried in fine-grained sediments. They concluded that sediment deposition appears to reflect major-scale-flooding events as would be expected from a strong seasonal variation in precipitation, probably with severe rainstorms after a dry period. The combined results of studies from micro- and megaplant fossils recorded from this formation in the Junggar Basin (Regional Stratigraphy of NW China, 1981) and its contemporary strata from northern China (Zhao, 1980) and Eurasia (Vakrhameev, 1991) all indicate a Middle to Late Jurassic climate that was arid to semiarid.

The annual climatic seasonality had a severe effect on tree growth, hence a considerable influence upon ontogenetic growth of dinosaurs may also be expected. The formation of LAGs may be explained by an interruption of bone growth due to environmental and nutritional stress during the dry season of the winter monsoon, with the metabolism of the dinosaur no longer being able to support a continuous growth of the bone. Restricted pasture and water supply is also compatible with higher $\delta^{18}O_p$ values for intervals containing LAGs (Figs. 5 and 6), as stronger evaporation is expected to increase the ^{18}O content of the surface waters.

Lower $\delta^{18}O_p$ values during growth intervals between LAGs (Fig. 6) also agree with a monsoon-type scenario as monsoon areas are commonly observed to have lower $\delta^{18}O_{H2O}$ values for summer precipitation compared to the winter precipitation despite higher summer temperatures. The reason for this is the so-called rainout effect during the wet monsoon season leading to relatively ^{18}O depleted precipitation (e.g., Rozanski et al., 1993).

Interestingly however, the bone histology of the two sympatric dinosaurs from the Junggar Basin indicates that they have reacted differently to the environmental stress that may have been caused by the monsoon climate: one periodically interrupted bone growth and formed multiple LAGs (Fig. 1a) while the others continued to form regular plexiform bone (Fig. 1b) without any histological features of limited bone growth. Similar observations have been made for different genera of dinosaurs from polar latitudes (Chinsamy et al., 1998). The fibrolamellar bone with the LAGs shows a cyclic intra-bone variability of the $\delta^{18}O_p$ values of 1.7 ‰ which is two times higher than that of the plexiform bone with ca. 0.8 ‰ This may hint towards species-specific differences in metabolic rate and thermophysiology. The higher intra-bone variability of $\delta^{18}O_p$ values as well as the 0.7 ‰ lower mean $\delta^{18}O_p$ value for the fibrolamellar bone with multiple LAGs compared to that of the plexiform sauropod bone without LAGs might indicate a more poikilothermic metabolism of this dinosaur. Lower ambient and body temperatures during the winter monsoon may have resulted in higher $\delta^{18}O_p$ values and a decrease in the metabolic activity below the threshold of bone growth, thus forming LAGs. In contrast, a more endothermic metabolism of the larger sauropod could cope with the seasonal temperature variation, keeping the body temperature more or less constant and resulting in a continuous bone growth and a low intra-bone variability of ≤ 0.8 ‰ similar to that of endotherm mammals and dinosaurs, including the sauropod *Camarasaurus* (Barrick and Showers, 1994; Barrick et al., 1997; Showers et al., 2002).

If thermophysiology and metabolic rate were similar in both dinosaurs, however, migration could be another explanation for the differences in bone histology and the intra-bone variation of the oxygen isotope composition. Large seasonal migrations over hundreds of kilometers or more due to seasonal climatic changes and deterioration of water and food resources are known from extant and extinct herbivorous mammals like wildebeest, zebras, reindeer, elephants, or mammoth (Koch et al., 1995; Hoppe et al., 1999; Wolanski et al., 1999), birds (Chamberlain et al., 1997), and may also have been possible for some dinosaurs (Parrish et al., 1987; Currie, 1989; Spotila et al., 1991). Migration should result in

reduced seasonality of the oxygen isotope compositions in the bone or tooth phosphate. The reason for that is that the migratory animals experience smaller seasonal temperature and/or humidity gradients, which reduces the amplitude of the seasonal variation of $\delta^{18}O$ values of meteoric and thus body water. The larger amplitude of intra-bone variation in the fibrolamellar bone and the formation of multiple LAGs indicate that this individual was exposed to more severe seasonal temperature and/or humidity variations. Thus this dinosaur can tentatively be interpreted as a local resident in the Junggar Basin with its strong monsoon climate. In contrast, the dinosaur with the plexiform bone without LAGs and a much lower intra-bone oxygen isotope variation might have escaped the severe monsoonal climate by migration. This would explain continuous bone growth and a low amplitude of intra-bone oxygen isotope variability. Differences in oxygen isotope composition of skeletal apatites from local individuals in comparison to those from different geographic or orographic origins and of different migratory habits have been observed for a number of mammals (e.g., Koch et al., 1995; White et al., 1998; Hoogewerff et al., 2001; Balasse et al., 2002; Müller et al., 2003).

5. Conclusions

Fossil bones of sympatric sauropods from the Junggar Basin display different styles of osteogenesis in their histology: (a) continuous bone growth of plexiform-type without the formation of LAGs, (b) periodic bone growth of fibrolamellar-type with multiple LAGs. These differences in bone histology and growth pattern are also reflected in different amplitudes and mean values of the oxygen isotope compositions of bone phosphate, indicating a causal link. Despite diagenetic alteration of REE and trace element contents the primary oxygen isotopic compositions and their pattern of cyclic intra-bone variation related to seasonal changes in ambient (body)temperatures and/or isotopic composition of drinking water can be preserved in Jurassic dinosaur bones. The differences in growth history and oxygen isotopic composition of the fibrolamellar and plexiform bones may indicate differences in thermophysiology or migrational movements of the sauropods.

The histology and changes in oxygen isotope compositions of the fibrolamellar bone with multiple LAGs of a Jurassic sauropod probably indicate annual growth cycles. These growth cycles may have been triggered by a seasonal monsoon-type climate that has also been suggested for fossil conifer wood samples from the Junggar Basin. This is evidence for a climatic influence on the growth of fibrolamellar bone in nonpolar dinosaurs and of cyclic intra-bone variation of $\delta^{18}O$ values.

Seasonal intra-bone variation of oxygen isotope compositions in fossil dinosaur bone that has not experienced extensive in vivo remodeling and diagenetic alteration might be used as annual time markers for skeletochronology and hence to quantify longevity and growth rates of dinosaurs. With this approach the assumed annual nature of histological growth marks like LAGs can be independently tested. Furthermore, seasonal intra-bone variation of $\delta^{18}O_p$ values potentially allows for estimates of growth rates, also for bones which do not show such LAGs.

Combined investigations of bone histology and high-resolution seasonal intra-bone variations of the oxygen isotopic compositions are promising, complementary methods that may help to constrain the skeletochronology, thermophysiology, metabolic rates as well as the potential influence of climate on these factors, giving new insights into the paleobiology of dinosaurs as well as other extant and extinct vertebrates.

Acknowledgements

We gratefully acknowledge the help of Gabi Stoscheck and Bernd Steinhilber for the isotopic analyses in the stable isotope laboratory at the Institut für Geowissenschaften of the University of Tübingen. We also thank Thomas Wenzel for his support during the electron microprobe analyses and Klaus Simon for making it possible to analyze the REE by LA-ICP-MS at the Zentrum für Geowissenschaften of the University of Göttingen. Our gratitude is also extended to the editor Bruce MacFadden who gave us the chance to submit this manuscript for publication as part of this special volume and for the efficient editorial handling. Finally, the fast, detailed and thoughtful reviews of Pennilyn Higgins and an anonymous reviewer im-

proved the quality of the manuscript significantly and are much appreciated. This study was part of a PhD thesis on bone diagenesis by Tütken, financed by grants PF 219/11-1+2 of the German National Science Foundation (DFG) to Pfretzschner and Vennemann.

References

Ayliffe, L.K., Chivas, A.R., Leakey, M.G., 1994. The retention of primary oxygen isotope compositions of fossil elephant skeletal phosphate. Geochim. Cosmochim. Acta 58, 5291–5298.

Balasse, M., Bocherens, H., Mariotti, A., 1999. Intra-bone variability of collagen and apatite isotopic composition used as evidence of a change of diet. J. Archaeol. Sci. 26, 593–598.

Balasse, M., Ambrose, S.H., Smith, A.B., Price, D., 2002. The seasonal mobility model for prehistoric herders in the southwestern Cape of South Africa assessed by isotopic analysis of sheep tooth enamel. J. Archaeol. Sci. 29, 917–932.

Barrick, R.E., Showers, W.J., 1994. Thermophysiology of *Tyrannosaurus rex*: evidence from oxygen isotopes. Science 265, 222–224.

Barrick, R.E., Showers, W.J., Fischer, A.G., 1996. Comparison of thermoregulation of four ornithischian dinosaurs and a varanid lizard from the Cretaceous two medicine formation; evidence from oxygen isotopes. Palaios 11, 295–305.

Barrick, R.E., Stoskopf, M.K., Showers, W.J., 1997. Oxygen isotopes in dinosaur bone. In: Farlow, J.O., Brett-Surman, M.K. (Eds.), The Complete Dinosaur. Indiana Univ. Press, Bloomington, IN, pp. 474–490.

Barrick, R.E., Patchus, R., Straight, R., Showers, W., Genna, W., 2001. Oxygen and carbon isotope evaluation of crocodilian tooth enamel: dietary and physiologic implications. J. Vertebr. Paleontol. 21 (Suppl. 3), A 32.

Blake, R.E., O'Neil, J.R., Garcia, G.A., 1997. Oxygen isotope systematics of biologically mediated reactions of phosphate: I. Microbial degradation of organophosporous compounds. Geochim. Cosmochim. Acta 61, 4411–4422.

Bligh, J., Johnson, K.G., 1973. Glossary of terms for thermal physiology. J. Appl. Physiol. 35, 661–941.

Bryant, J.D., Froelich, P.N., 1995. A model of oxygen isotope fractionation in body water of large mammals. Geochim. Cosmochim. Acta 60, 4523–4537.

Bryant, J.D., Froelich, P.N., Showers, W.J., Genna, B.J., 1996a. Biologic and climatic signals in the oxygen isotopic composition of Eocene–Oligocene equid enamel phosphate. Palaeogeogr. Palaeoclimatol. Palaeoecol. 126, 75–89.

Bryant, J.D., Koch, P.L., Froelich, P.N., Showers, W.J., Genna, B.J., 1996b. Oxygen isotope partitioning between phosphate and carbonate in mammalian apatite. Geochim. Cosmochim. Acta 60, 5145–5148.

Buffrénil, V. de, 1982. Données preliminaries sur la présence de lignes d'arrêt de croissance périostiques dans la mandibule du marouin commun, *Phocoena phocoena*, (L.), et leur utilisation comme indicateur de l'âge. Can. J. Zool. 60, 2557–2567.

Buffrénil, V. de, Buffetaut, E., 1981. Skeletal growth lines in an Eocene crododilian skull from Wyoming as an indicator of ontogenetic age and paleoclimatic conditions. J. Vertebr. Paleontol. 1, 57–66.

Buffrénil, V. de, Farlow, J.O., de Ricqlés, A., 1986. Growth and function of Stegosaurus plates: evidence from bone histology. Paleobiology 12, 459–473.

Castanet, J., Smirina, E., 1990. Introduction to the skeletochronological method in amphibians and reptiles. Ann. Sci. Nat. Zool. (Paris) 13 (Série 11), 191–196.

Castanet, J., Francillon-Vieillot, H., Meuner, F.J., de Ricqlès, A., 1993. Bone and individual aging. In: Hall, B.K. (Ed.), Bone. Bone Growth-B, vol. 7. CRC Press, Boca Raton, pp. 245–283.

Chamberlain, C.P., Blum, J.D., Holmes, R.T., Feng, X., Sherry, T.W., Graves, G.R., 1997. The use of isotope tracers for identifying populations of migratory birds. Oecologia 109, 132–141.

Chinsamy, A., 1990. Physiological implications of the bone histology of *Syntarsus rhodesiensis* (Saurischia: Theropoda). Paleontolo. Afr. 27, 77–82.

Chinsamy, A., 1995. Ontogenetic changes in the bone histology of the Late Jurassic ornithopod *Dryosaurus lettowvorbecki*. J. Vertebr. Paleontol. 15, 96–104.

Chinsamy, A., Rich, T., Vickers-Rich, P., 1998. Polar dinosaur bone histology. J. Vertebr. Paleontol. 18, 385–390.

Currie, P.J., 1989. Long distance dinosaurs. Nat. Hist. 6/89, 60–65.

Currie, P.J., Zhao, X.-J., 1993. A new carnosaur form (Dinosauria, Theropoda) from the Jurassic of Xinjiang, People's Republic of China. Can. J. Earth Sci. 30, 2037–2081.

Curry, K.A., 1999. Ontogenetic histology of *Apatosaurus* (Dinosauria: Sauropoda): new insights on growth rates and longevity. J. Vertebr. Paleontol. 19, 654–665.

Dansgaard, W., 1964. Stable isotopes in precipitation. Tellus 16, 436–468.

Dong, Z.M., 1989. On a small ornithopod (*Gangbusaurus wucaiwanensis*) form Kelamaili, Junggar Basin, Xinjiang, China. Vertebrata Palasiatica 27, 140–146.

Dong, Z.M., 1992. Dinosaurian Faunas of China. China Ocean Press, Springer-Verlag.

Elzora, J., Astibia, H., Murelaga, X., Pereda-Suberbiola, X., 1999. Francolite as a diagenetic mineral in dinosaur and other Upper Cretaceous reptile bones (Lano, Iberian Peninsula): microstructural, petrological and geochemical features. Cretac. Res. 20, 169–187.

Enlow, D.H., 1963. Principles of Bone Remodeling. Charles C. Thomas, Springfield.

Erickson, G.M., Tumanova, T.A., 2000. Growth curve of *Psittacosaurus mongolensis* Osborn (Ceratopsia: Psittacosauridae) inferred form long bone histology. Zool. J. Linn. Soc. 130, 551–556.

Erickson, G.M., Rogers, K.C., Yerby, S.A., 2001. Dinosaurian growth patterns and rapid avian growth rates. Nature 412, 429–433.

Farlow, J.O., Brett-Surman, M.K., 1997. The Complete Dinosaur Indiana Univ. Press, Bloomington, IN.

Francillon-Vieillot, H., de Buffrénil, V., Castanet, J., Geraudie, J., Meunier, F.J., Sire, J.Y., Zylberg, L., de Ricqlès, A., 1990. Microstructures and mineralization of vertebrate skeletal tis-

sues. In: Carter, J.G. (Ed.), Biomineralization: Patterns and Evolutionary Trends. Van Nostrand Reinhold, New York, pp. 471–530.

Francis, J.E., 1984. The seasonal environment of the Purbeck (Upper Jurassic) fossil forests. Palaeogeogr. Palaeoclimatol. Palaeoecol. 48, 285–301.

Fricke, H.C., O'Neil, J.R., 1996. Inter- and intra-tooth variation in the oxygen isotope composition of mammalian tooth enamel phosphate; implications for palaeoclimatological and palaeobiological research. Palaeogeogr. Palaeoclimatol. Palaeoecol. 126, 91–96.

Fricke, H.C., O'Neil, J.R., 1999. The correlation between $^{18}O/^{16}O$ ratios of meteoric water and surface temperature: its use in investigating terrestrial climate change over geologic time. Earth Planet. Sci. Lett. 170, 181–196.

Fricke, H.C., Rogers, R.R., 2000. Multiple taxon-multiple locality approach to providing oxygen isotope evidence for warm-blooded theropod dinosaurs. Geology 28, 799–802.

Fricke, H.C., Clyde, W.C., O'Neil, J.R., 1998. Intra-tooth variations in $\delta^{18}O$ (PO_4) of mammalian tooth enamel as a record of seasonal variations in continental climate variables. Geochim. Cosmochim. Acta 62, 1839–1850.

Frost, H.M., 1980. Skeletal physiology and bone remodeling. In: Urist, M.R. (Ed.), Fundamentals and Clinical Bone Physiology. J.B. Lippincott, Philadelphia, pp. 208–241.

Hancox, N.M., 1972. The Biology of Bone. Cambridge Univ. Press, Cambridge.

Hendrix, M.S., Graham, S.A., Carroll, A.R., Soebel, E.R., McKnight, C.L., Schulein, B.J., Wang, Z., 1992. Sedimentary record and climate implications of recurrent deformation in the Tian Shan: evidence from Mesozoic strata of the north Tarim, south Junggar, and Turpan basins, northwest China. Geol. Soc. Amer. Bull. 104, 53–79.

Hoogewerff, J., Papesch, W., Kralik, M., Berner, M., Vroon, P., Miesbauer, H., Gaber, O., Künzel, K.H., Kleinjans, J., 2001. The last domicile of the Iceman from Hauslabjoch: a geochemical approach using Sr, C and O isotopes and trace element signatures. J. Archaeol. Sci. 28, 983–989.

Hoppe, K.A., Koch, P.L., Carlson, R.W., Webb, S.D., 1999. Tracking mammoths and mastodons; reconstruction of migratory behavior using strontium isotope ratios. Geology 27, 439–442.

Horner, J.R., Currie, P.J., 1994. Embryonic and neonatal morphology and ontogeny of a new species of Hypacrosaurus (Ornitischia, Lambeosauridae) from Montana and Alberta. In: Carpenter, K., Hirsch, K.F., Horner, J.R. (Eds.), Dinosaur Eggs and Babies. Cambridge Univ. Press, Cambridge, UK, pp. 347–365.

Horner, J.R., Padian, K., de Ricqlès, A., 1997. Histological analysis of a dinosaur skeleton: evidence of skeletal growth variation. J. Morphol. 232, 267 A.

Horner, J.R., de Ricqlès, A., Padian, K., 1999. Variation in dinosaur skeletochronology indicators: implications for age assessment and physiology. Paleobiology 25, 295–304.

Horner, J.R., de Ricqlès, A., Padian, K., 2000. Long bone histology of the hadrosaurid dinosaur *Maiasaura peeblesorum*: growth dynamics and physiology based on an ontogenetic series of skeletal elements. J. Vertebr. Paleontol. 20, 115–129.

Hubert, J.F., Panish, P.T., Chure, D.J., Prostak, K.S., 1996. Chemistry, microstructure, petrology and diagenetic model of Jurassic dinosaur bones, Dinosaur National Monument, Utah. J. Sediment. Res. 66, 531–547.

Hutton, J.M., 1986. Age determination of living Nile crocodiles from the cortical stratification of bone. Copeia 2, 332–341.

Iacumin, P., Bocherens, H., Mariotti, A., Longinelli, A., 1996. Oxygen isotope analyses of co-existing carbonate and phosphate in biogenic apatite; a way to monitor diagenetic alteration of bone phosphate? Earth Planet. Sci. Lett. 142, 1–6.

Jee, W.S.S., 1988. The skeletal tissues. In: Weiss, L. (Ed.), Cell and Tissue Biology, 6 ed., Urban and Schwarzberg, München, pp. 213–254.

Jensen, M., Sharp, Z., Atudoeri, V., 1999. Evidence for primary oxygen isotope composition in dinosaur tooth enamel: implications for physiology and behavior. Abstr. Programs-Geol. Soc. Am. Annu. Meet. 31, A 97.

Keller, A.M., Hendrix, M.S., 1997. Paleoclimatologic analysis of a Late Jurassic petrified forest, southeastern Mongolia. Palaios 12, 282–291.

Klevezal, G.A., 1996. Recording structures of mammals, determination of age and reconstruction of live history. A.A. Balkema, Rotterdam.

Klevezal, G.A., Kleinenberg, S.E., 1967. Age determination of mammals from the layered structures in teeth and bones (in Russian) Nauka, Moscow, English Translation by J. Salkind, (1969). Israel Program for Scientific Translations, Jerusalem.

Koch, P.L., 1998. Isotopic reconstruction of past continental environments. Annu. Rev. Earth Planet. Sci. 26, 573–613.

Koch, P.L., Fisher, D.C., Dettman, D.L., 1989. Oxygen isotopic variation in the tusks of extinct proboscideans; a measure of season of death and seasonality. Geology 17, 515–519.

Koch, P.L., Fogel, M.L., Tuross, N., 1994. Tracing the diet of fossil animals using stable isotopes. In: Lajtha, K., Michener, R.H. (Eds.), Stable Isotopes in Ecology and Environmental Science. Blackwell Scientific Publication, Oxford, pp. 63–93.

Koch, P.L., Heisinger, J., Moss, C., Carlson, R.W., Fogel, M.L., Behrensmeyer, A.K., 1995. Isotopic tracking of the diet and habitat use in African elephants. Science 267, 1340–1343.

Koch, P.L., Tuross, N., Fogel, M.L., 1997. The effects of sample treatment and diagenesis on the isotopic integrity of carbonate in biogenic hydroxylapatite. J. Archaeol. Sci. 24, 417–429.

Kohn, M.J., 1996. Predicting animal $\delta^{18}O$: accounting for diet and physiological adaptation. Geochim. Cosmochim. Acta 60, 4811–4829.

Kohn, M.J., Cerling, T.E., 2002. Stable isotope compositions of biological apatite. In: Kohn, M.J., Rakovan, J., Hughes, J.M. (Eds.), Phosphates: Geochemical, Geobiological, and Materials Importance. Rev. Mineral. Geochem., vol. 48, pp. 455–488.

Kohn, M.J., Schoeninger, M.J., Valley, J.W., 1998. Variability in oxygen isotope compositions of herbivore teeth; reflections of seasonality or developmental physiology? Chem. Geol. 152, 97–112.

Kohn, M.J., Schoeninger, M.J., Barker, W.B., 1999. Altered states: effects of diagenesis on fossil tooth chemistry. Geochim. Cosmochim. Acta 63, 2737–2747.

Kolodny, Y., Luz, B., Navon, O., 1983. Oxygen isotope variations

in phosphate of biogenic apatites: I. Fish bone apatite; rechecking the rules of the game. Earth Planet. Sci. Lett. 64, 398–404.
Kolodny, Y., Luz, B., Sander, M.W., Clemens, A., 1996. Dinosaur bones: fossils or pseudomorphs? The pitfalls of physiology reconstruction from apatitic fossils. Palaeogeogr. Palaeoclimatol. Palaeoecol. 126, 161–171.
Kutzbach, J.E., Gallimore, R.G., 1989. Pangean climates: megamonsoon of the megacontinent. J. Geophys. Res. 94, 3341–3357.
Lockley, M.G., 1994. Dinosaur ontogeny and population structure: interpretations and speculations based on fossil footprints. In: Carpenter, K., Currie, P.J. (Eds.), Dinosaur Systematics: Approaches and Perspectives. Cambridge Univ. Press, Cambridge, UK, pp. 211–220.
Longinelli, A., 1984. Oxygen isotopes in mammal bone phosphate; a new tool for paleohydrological and paleoclimatological research? Geochim. Cosmochim. Acta 48, 385–390.
Longinelli, A., 1995. Stable isotope ratios in phosphate in mammal bone and tooth as climatic indicators. In: Frenzel, B., Stauffer, B., Weiß, M.M. (Eds.), Problems of Stable Isotopes in Tree Rings, Lake Sediments and Peat Bogs as Climatic Evidence for the Holocene. Fischer, Stuttgart, pp. 58–70.
Longinelli, A., Nuti, S., 1973. Revised phosphate-water isotopic temperature scale. Earth Planet. Sci. Lett. 19, 373–376.
Loope, D.B., Rowe, C.M., Joeckel, R.M., 2001. Annual monsoon rains recorded by Jurassic dunes. Nature 412, 64–66.
Lucas, J., Prevot, L.E., 1991. Phosphates and fossil preservation. In: Allison, P.A., Briggs, D.E.G. (Eds.), Taphonomy. Plenum, New York, pp. 389–409.
Luz, B., Kolodny, Y., 1985. Oxygen isotope variations in phosphate of biogenic apatites: IV. Mammal teeth and bones. Earth Planet. Sci. Lett. 75, 29–36.
Luz, B., Kolodny, Y., 1989. Oxygen isotope variation in bone phosphate. Appl. Geochem. 4, 317–323.
Luz, B., Kolodny, Y., Horowitz, M., 1984. Fractionation of oxygen isotopes between mammalian bone-phosphate and environmental drinking water. Geochim. Cosmochim. Acta 48, 1689–1693.
McKnight, C.L., Graham, S.A., Carroll, A.R., Gan, Q., Dilcher, D.L., Zhao, M., Yun, H.L., 1990. Fluvial sedimentology of an Upper Jurassic petrified forest assemblage, Shishu Formation, Junggar Basin, Xinjiang, China. Palaeogeogr. Palaeoclimatol. Palaeoecol. 79, 1–9.
Müller, W., Fricke, H., Halliday, A.N., McCulloch, M.T., Wartho, J.-A., 2003. Origin and migration of the Alpine Iceman. Science 302, 162–166.
Nelson, B.K., DeNiro, M.J., Schoeninger, M.J., DePaolo, D.J., Hare, P.E., 1986. Effects of diagenesis on strontium, carbon, nitrogen and oxygen concentration and isotopic composition of bone. Geochim. Cosmochim. Acta 50, 1941–1949.
O'Neil, J.R., Roe, L.J., Reinhard, E., Blake, R., 1994. A rapid and precise method of oxygen isotope analysis of biogenic phosphate. Isr. J. Earth-Sci. 43, 203–212.
Padian, K., 1997. Growth lines. In: Currie, P.J., Padian, K. (Eds.), Encyclopedia of Dinosaurs. Academic Press, San Diego, pp. 288–291.
Padian, K., de Riqlès, A.J., Horner, J.H., 2001. Dinosaurian growth rates and bird origin. Nature 412, 405–408.
Parrish, J.T., Ziegler, A.M., Scotese, C.R., 1982. Rainfall patterns and the distribution of coals and evaporates in the Mesozoic and Cenozoic. Palaeogeogr. Palaeoclimatol. Palaeoecol. 40, 67–101.
Parrish, J.M., Parrish, J.T., Hutchinson, J.H., Spicer, R.A., 1987. Late Cretaceous vertebrate fossils from the north slope of Alaska and implications for dinosaur ecology. Palaios 2, 377–389.
Passey, B.H., Cerling, T.E., 2002. Tooth mineralization in ungulates: implications for recovering a primary isotopic time-series. Geochim. Cosmochim. Acta 66, 3225–3234.
Peabody, F.E., 1958. A Kansas drought record in growth zones of a bullsnake. Copeia 2, 91–94.
Peabody, F.E., 1961. Annual growth zones in living and fossil vertebrates. J. Morphol. 108, 11–62.
Pflug, K.P., Schuster, K.D., Pichotka, J.P., Forstel, H., 1979. Fractionation effects of oxygen isotopes in mammals. In: Klein, E.R., Klein, P.D. (Eds.), Stable Isotopes: Proceedings of the Third International Conference. Academic Press, New York, pp. 553–561.
Pfretzschner, H.-U., Ashraf, A.R., Maisch, M.W., Sun, G., Wang, Y., Mosbrugger, V., 2001. Cyclic growth in dinosaur bones from the upper Jurassic of NW China and its paleoclimatic implications. Proceedings of the Sino-Germany Symposium on Prehistory life and Geology of Junggar Basin. Xinjiang, Urumqi, pp. 21–39.
Regional Stratigraphy of NW China, 1981. Xinjiang, Stratigraphic Committee of Xinjiang. Geol. Publ. House, Beijing.
Reid, R.E.H., 1981. Lamellar-zonal bone with zones and annuli in the pelvis of a sauropod dinosaur. Nature 292, 49–51.
Reid, R.E.H., 1990. Zonal "growth rings" in dinosaurs. Mod. Geol. 15, 19–48.
Reid, R.E.H., 1997a. How dinosaurs grew. In: Farlow, J.O., Brett-Surman, M.K. (Eds.), The Complete Dinosaur. Indiana Univ. Press, Bloomington, IN, pp. 403–413.
Reid, R.E.H., 1997b. Dinosaurian physiology: the case for "intermediate dinosaurs". In: Farlow, J.O., Brett-Surman, M.K. (Eds.), The Complete Dinosaur. Indiana Univ. Press, Bloomington, IN, pp. 449–473.
Ricqlès, A. de, 1974. The evolution of endothermy: histological evidence. Evol. Theory 1, 51–80.
Ricqlès, A. de, 1980. Tissue structure of dinosaur bone: functional significance and possible relation to dinosaur physiology. In: Thomas, R.D.K., Olson, E.C. (Eds.), A Cold Look at Warm Blooded Dinosaurs. AAAS Selected Symposium, vol. 28. Westview Press, Boulder, pp. 103–139.
Ricqlès, A. de, 1983. Cyclical growth in the long limb bones of a sauropod dinosaur. Acta Palaeontol. Pol. 28, 225–232.
Ricqlès, A. de, Meunier, F.J., Castanet, J., Francillon-Vieillot, H., 1991. Comparative microstructure of bone. In: Hall, B.K. (Ed.), Bone. Bone Matrix and Bone Specific Products, vol. 3. CRC Press, Boca Raton, pp. 1–78.
Ricqlès, A. de, Horner, J.R., Padian, K., 1998. Growth dynamics of the hadrosaurid dinosaur Maiasaura peeblesorum. J. Vertebr. Paleontol. 18 (Suppl. 3), 72A.
Rozanski, K., Araguás-Araguás, L., Gonfiantini, R., 1993. Isotopic patterns in modern global precipitation. In: Swart, P.K, Lohmann, K.C, McKenzie, J.A., Savin, S. (Eds.), Climate Change in Continental Isotopic Records. Geophys. Monogr. Ser., vol. 78. Am. Geophys. Union, Washington D.C., pp. 1–36.

Russell, D.A., Zheng, Z., 1993. A large mamenchisaurid from the Junggar Basin, Xinjiang, People's Republic of China. Can. J. Earth Sci. 30, 2082–2095.

Sander, P.M., 1999. Life history of Tendaguru sauropods as inferred from long bone histology. Mitteilungen des Museums für Naturkunde Berlin. Mitt. Muss. Naturkd. Berlin, Geowiss. Reihe 2, 103–112.

Sander, P.M., 2000. Long bone histology of the Tendaguru sauropods: implications for growth and biology. Paleobiology 26, 466–488.

Sander, P.M., Tückmantel, C., 2003. Bone lamina thickness, bone apposition rates, and age estimates in sauropod humeri and femora. Paläontol. Z. 76, 161–172.

Schoeller, D., Leitch, C., Brown, C., 1986. Doubly labeled water method: in vivo oxygen and hydrogen isotope fractionation. Am. J. Physiol. 251, 1137–1143.

Scotese, C.R., 1999. Digital Paleogeographic Map Archive on CD-ROM, PALEOMAP Project, Arlington, Texas.

Sereno, P.C., 1999. The evolution of dinosaurs. Science 284, 2137–2147.

Sharp, Z.D., Cerling, T.E., 1998. Fossil isotope records of seasonal climate and ecology: straight from the horse's mouth. Geology 26, 219–222.

Showers, W.J., Reese, B., Genna, B., 2002. Isotopic analysis of dinosaur bones—a new pyrolysis technique provides direct evidence that some dinosaurs were warm-blooded. Anal. Chem. 74, 143–150.

Spotila, J.R., O'Connor, M.P., Dodson, P., Paladino, F.V., 1991. Hot and cold running dinosaurs: body size, metabolism, and migration. Mod. Geol. 16, 202–227.

Stephan, E., 1999. Sauerstoffisotopenverhältnisse im Knochengewebe großer terrestrischer Säugetiere. Tüb. Geowiss. Arb. 6, 1–218.

Stephan, E., 2000. Oxygen isotope analysis of animal bone phosphate: method refinement, influence of consolidants, and reconstruction of palaeotemperatures for Holocene sites. J. Archaeol. Sci. 27, 523–535.

Stoskopf, M.K., Barrick, R.E., Showers, W.J., 2001. Oxygen isotope variability in bones of wild caught and constant temperature reared sub-adult America alligators. J. Therm. Biol. 26, 183–191.

Straight, W., Barrick, R.E., Showers, W.J., Russel, D.A., 1999. Paleoclimatologic and paleobiologic utility of stable isotope records preserved in large theropod dinosaur teeth. Abstr. Programs-Geol. Soc. Am. Annu. Meet. 31, A 356.

Tang, Z., Parnell, L., Longstaffe, F.J., 1997. Diagenesis and reservoir potential of Permian–Triassic fluviatil/lacustrine sandstones in the southern Junggar Basin, northwestern China. AAPG Bull. 81, 1843–1865.

Thomas, K.J., Carlson, S.J., 2001. Examination of enamel growth rates in the Hadrosaurian dinosaur Edmontosaurus using oxygen isotope variability. Abstr. Programs-Geol. Soc. Am. Annu. Meet. 33, A 114.

Trueman, C.N., Martill, D.M., 2002. The long-term survival of bone: the role of bioerosion. Archaeometry 44, 371–382.

Trueman, C.N., Tuross, N., 2002. Trace elements in recent and fossil bone apatite. In: Kohn, M.J., Rakovan, J., Hughes, J.M. (Eds.), Phosphates: Geochemical, Geobiological, and Materials Importance. Rev. Mineral. Geochem., vol. 48. pp. 489–521.

Tütken, T., 2003. Die Bedeutung der Knochenfrühdiagenese für die Erhaltungsfähigkeit in vivo erworbener Element-und Isotopenzusammensetzungen in fossilen Knochen. PhD thesis, University of Tübingen, Germany, http://w210.ub.uni-tuebingen.de/dbt/volltexte/2003/962/.

Tütken, T., Vennemann, T.W., Pfretzschner, H.-U., 2001. Diagenetic alteration of biogenic phosphate—constraints from oxygen isotope analysis of vertebrate fossils from Neogene marine deposits. J. Conf. Abstr. 6, 500.

Tütken, T., Kuznetsova, T.V., Vennemann, T.W., Pfretzschner, H.-U., 2002. Late Pleistocene–Holocene climate of Siberia deduced from oxygen isotope compositions of mammoth and horse bone phosphate. Geochim. Cosmochim. Acta 66 (S 1), A 885.

Vakrhameev, V.A., 1991. Jurassic and Cretaceous Floras and Climates of the Earth. Cambridge Univ. Press, Cambridge.

Varricchio, D.J., 1993. Bone microstructure of the Upper Cretaceous theropod dinosaur *Troodon formosus*. J. Vertebr. Paleontol. 13, 99–104.

Varricchio, D.J., 1997. Growth and embryology. In: Currie, P.J., Padian, K. (Eds.), Encyclopedia of Dinosaurs. Academic Press, San Diego, pp. 282–288.

Vennemann, T.W., Fricke, H.C., Blake, R.E., O'Neil, J.R., Colman, A., 2002. Oxygen isotope analysis of phosphates: a comparison of techniques for analysis of Ag_3PO_4. Chem. Geol. 185, 321–336.

Wang, Y.D., Zhang, W., Saiki, K., 2000. Fossil woods from the Upper Jurassic of Qitai, Junggar Basin, Xinjiang, China. Acta Palaeontol. Sin. 39, 176–185.

White, C.D., Spence, M.W., Stuart-Williams, H.L.Q., Schwarcz, H.P., 1998. Oxygen isotopes and the identification of geographical origins: the Valley of Oaxaca versus the Valley of Teotihuacan. J. Archaeol. Sci. 25, 643–655.

Wilkinson, B.H., Ivany, L.C., 2002. Paleoclimatic inference from stable isotope profiles of accretionary biogenic hardparts—a quantitative approach to the evaluation of incomplete data. Palaeogeogr. Palaeoclimatol. Palaeoecol. 185, 95–114.

Wolanski, E., Gereta, E., Borner, M., Mduma, S., 1999. Water, migration and the Serengeti ecosystem. Am. Sci. 87, 526–533.

Wong, W.W., Cochran, W.J., Klish, W.J., Smith, E.O., Lee, L.S., Klein, P.D., 1988. In vivo isotope-fractionation factors and the measurement of deuterium and oxygen-18 dilution spaces from plasma, urine, saliva, respiratory water vapor and carbon dioxide. Am. J. Clin. Nutr. 47, 1–6.

Zhao, X., 1980. Mesozoic vertebrate-bearing beds and stratigraphy of northern Xinjiang. Mem. Inst. Vertebr. Paleontol. Paleoanthropol. Acad. Sin. A 16. 160 pp.

Zhiyi, Z., Dean, W.T., 1996. Phanerozoic Geology of Northwest China. VSP International Science Publishers, Utrecht.

Zocco, T.G., Schwartz, H.L., 1994. Microstructural analysis of bone of the sauropod dinosaur Seismosaurus by transmission electron microscopy. Palaeontology 37, 493–503.